Insights into the structure and function of H_V1 from a meta-analysis of mutation studies

Thomas E. DeCoursey,[1] Deri Morgan,[1] Boris Musset,[2] and Vladimir V. Cherny[1]

[1]Department of Molecular Biophysics and Physiology, Rush University, Chicago, IL 60612
[2]Institut für Physiologie, PMU Klinikum Nürnberg, 90419 Nürnberg, Germany

The voltage-gated proton channel (H_V1) is a widely distributed, proton-specific ion channel with unique properties. Since 2006, when genes for H_V1 were identified, a vast array of mutations have been generated and characterized. Accessing this potentially useful resource is hindered, however, by the sheer number of mutations and interspecies differences in amino acid numbering. This review organizes all existing information in a logical manner to allow swift identification of studies that have characterized any particular mutation. Although much can be gained from this meta-analysis, important questions about the inner workings of H_V1 await future revelation.

The Journal of General Physiology

Introduction

Voltage-gated proton channels are found in highly diverse species, from unicellular marine creatures such as dinoflagellates, diatoms, and coccolithophores (Smith et al., 2011; Taylor et al., 2011, 2012) to insects (Chaves et al., 2016), snails (Thomas and Meech, 1982; Byerly et al., 1984; Doroshenko et al., 1986), and human beings, where they are found in a variety of cells and perform many disparate functions (DeCoursey, 2013). Their unique properties (perfect H^+ selectivity, ΔpH-dependent gating, extreme temperature dependence, and the ability to shift into a strikingly enhanced gating mode) are paralleled by a unique structure, the reconciliation of which is a goal of this review. Most voltage-gated ion channels are tetramers or quasi-tetramers of monomers comprising a voltage-sensing domain (VSD) S1–S4 (transmembrane [TM] segments 1–4) and a pore domain S5–S6, four of which combine to produce a single central conduction pathway. In contrast, H_V1 consists of S1–S4 alone, a VSD without an explicit pore domain (Ramsey et al., 2006; Sasaki et al., 2006). In mammals and many other species (Koch et al., 2008; Lee et al., 2008; Tombola et al., 2008; Smith and DeCoursey, 2013), H_V1 forms a dimer in cell membranes. However, each monomer, or protomer, has its own pore and other necessary parts and can function as a monomer (Koch et al., 2008; Tombola et al., 2008). The properties of monomeric constructs are similar in most respects to those of the dimer, but monomeric constructs open faster (Koch et al., 2008; Tombola et al., 2008; Musset et al., 2010b,c; Fujiwara et al., 2012). Several lines of evidence indicate that the two protomers comprising the H_V1 dimer do not function independently, but gate cooperatively in the sense that each must undergo a voltage-dependent conformational change before either can conduct current (Gonzalez et al., 2010; Musset et al., 2010b; Tombola et al., 2010; Smith and DeCoursey, 2013).

Fig. 1 illustrates schematically the entire 273–amino acid sequence of hH_V1. The signature sequence that has been used successfully to identify H_V1 in new species is RxWRxxR in the S4 helix (Smith et al., 2011; Rodriguez et al., 2015; Chaves et al., 2016). This sequence also identifies c15orf27 proteins, of unknown function, but these all lack Asp^{112} in S1, which is required for proton selectivity (Table 1). Another reported conserved motif in S2, [F,Y,W]xx[E,D]xxx[R,K], identifies some H_V1 channels but is not specific to H_V1, and instead identifies VSDs in general (Kang and Baker, 2016). This motif is not present in all H_V1; for example, it is not present in several unicellular marine species (Taylor et al., 2011), including kH_V1, which was identified by using the S4 motif (Smith et al., 2011).

Many reviews describe in detail the biological functions proposed for H_V1 (Eder and DeCoursey, 2001; DeCoursey, 2010, 2012, 2013; Capasso et al., 2011; Demaurex, 2012; Fischer, 2012; Lishko et al., 2012; Taylor et al., 2012; Smith and DeCoursey, 2013; DeCoursey and Hosler, 2014; Seredenina et al., 2015). Here we will summarize a few aspects of functions that are relevant to the analysis that follows. The main function of H_V1 in most cells is acid extrusion, although the specific consequences in each cell vary drastically. For example, H_V1-mediated acid extrusion triggers capacitation in human sperm (Lishko et al., 2010), enables histamine release by basophils (Musset et al., 2008b), and exacerbates several cancers (Wang et al., 2012, 2013; Hondares et al., 2014). Acid extrusion requires extreme proton selectivity because the concentration of H^+ in biological solutions is a million-fold lower than that of other major ions. H_V1 are

Correspondence to Thomas E. DeCoursey: tdecours@rush.edu

Abbreviations used: EPR, electron paramagnetic resonance; MD, molecular dynamics; NADPH, nicotinamide adenine dinucleotide phosphate; NEM, *n*-ethylmaleimide; TM, transmembrane; VSD, voltage-sensing domain.

© 2016 DeCoursey et al. This article is distributed under the terms of an Attribution–Noncommercial–Share Alike–No Mirror Sites license for the first six months after the publication date (see http://www.rupress.org/terms). After six months it is available under a Creative Commons License (Attribution–Noncommercial–Share Alike 3.0 Unported license, as described at http://creativecommons.org/licenses/by-nc-sa/3.0/).

The Rockefeller University Press $30.00
J. Gen. Physiol. 2016 Vol. 148 No. 2 97–118
www.jgp.org/cgi/doi/10.1085/jgp.201611619

CrossMark

Downloaded from http://rupress.org/jgp/article-pdf/148/2/97/1795854/jgp_201611619.pdf by guest on 08 February 2026

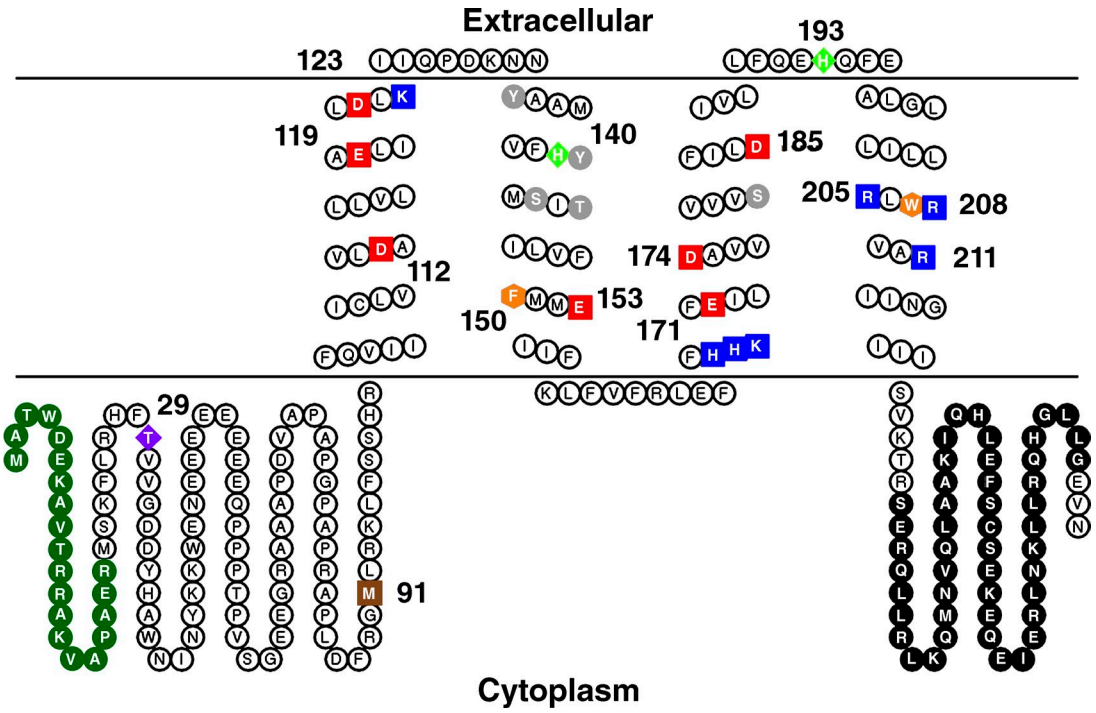

Figure 1. **The amino acid sequence and schematic topology of the human voltage-gated proton channel, hH_V1.** Within the TM domain, acidic residues are red, basic residues are blue, aromatic residues are orange, and polar residues are gray. Specific amino acids of note, beginning at the N terminus: deletion of 1–20 (green) produces a "short" isoform common in malignant B cells (Hondares et al., 2014); Thr^{29} is a PKC phosphorylation site responsible for enhanced gating (Musset et al., 2010a); M91T is the first identified hH_V1 mutation (Iovannisci et al., 2010); Asp^{112} is crucial to H^+ selectivity (Musset et al., 2011); His^{140} and His^{193} coordinate Zn^{2+} binding (Ramsey et al., 2006); the three Arg in S4 are thought to open the conductance pathway in response to voltage (Ramsey et al., 2006; Sasaki et al., 2006; Gonzalez et al., 2013); and the C terminus has an extensive coiled-coil region (black) that holds the dimer together (Koch et al., 2008; Lee et al., 2008; Tombola et al., 2008; Fujiwara et al., 2014). The image was drawn with TOPO2 (Johns, 2016).

brilliantly designed and extremely efficient acid extrusion devices, changing pH_i at least an order of magnitude faster than other H^+ exporters (DeCoursey and Cherny, 1994), mainly because of their unique ΔpH-dependent gating mechanism (Cherny et al., 1995), which is discussed in detail below in the section Table entries defined. A second type of function of H_V1 in many cells reflects the electrical consequences of the charge movement that occurs during H^+ extrusion. For example, in phagocytes and certain other cells, H^+ efflux serves to compensate electrically for the electron extrusion that occurs as a direct consequence of the electrogenic activity of nicotinamide adenine dinucleotide phosphate (NADPH; reduced form) oxidase and related NOX (cytochrome subunit of NADPH oxidase) isoforms (Henderson et al., 1987, 1988; DeCoursey et al., 2003). In dinoflagellates, H_V1 are thought to mediate the action potential that triggers the flash in bioluminescent species (Smith et al., 2011; Taylor et al., 2012).

The respiratory burst of phagocytes, which can be elicited by pathogenic microbes, chemotactic peptides, or the phorbol ester PMA, is the manifestation of NAD PH oxidase activation. During the respiratory burst, H_V1 properties undergo a drastic transformation (Bánfi et al., 1999; DeCoursey et al., 2000; Murphy and DeCoursey, 2006; DeCoursey, 2016), resulting in a much higher level of activity in what has been called the enhanced gating mode (DeCoursey, 2003b). The bulk of evidence indicates that enhanced gating results from phosphorylation of H_V1 (Morgan et al., 2007, Musset et al., 2010a; DeCoursey, 2016); mutations to putative phosphorylation sites are listed in Table 2.

Table 1 presents the position numbers of several key amino acids in H_V1 from the nine species in which the channel has been verified by electrophysiological studies in heterologous expression systems, and the corresponding positions in two closely related molecules (c15orf27 and CiVSP) as well as in two exhaustively studied K^+ channels. H_V1 contains two highly conserved Asp that other voltage-gated ion channels lack, Asp^{112} and Asp^{185}, as well as an anomalously located Trp^{207}. However, H_V1 lack the equivalent of Glu^{283} of *Shaker* and Na^+ channels, having Ser^{143} instead.

Fig. 2 shows where several key amino acids are located in the closed crystal structure of a mouse H_V1 (mH_V1) chimera (Fig. 2 A; Takeshita et al., 2014) and an open state model of hH_V1 (Fig. 2 B; Kulleperuma et al., 2013).

Downloaded from http://rupress.org/jgp/article-pdf/148/2/97/1795854/jgp_201611619.pdf by guest on 08 February 2026

Table 1. **Numerical key to H_V1 in species verified by heterologous expression**

	S1					S2				S3				S4				
Species	**HG**	**Sel**				**Zn^{2+}**	**HG**					**HG**						
hH_V1	**V109**	**D112**	E119	D123	K125	H140	**F150**	E153	K157	E171	D174	**V178**	D185	**R205**	W207	**R208**	**R211**	N214
mH_V1	**V105**	**D108**	E115	D119	K121	H136	**F146**	E149	K153	E167	D170	**V174**	D181	**R201**	W203	**R204**	**R207**	N210
CiH_V1	**V157**	**D160**	E167	D171	K173	H188	**F198**	E201	K205	E219	D222	**V226**	D233	**R255**	W257	**R258**	**R261**	N264
NpH_V1	**V63**	**D66**	E73	D77	E79	H92	**F102**	E105	K109	E123	D126	**V130**	D137	**R157**	W159	**R160**	**R163**	N166
SpH_V1	**V70**	**D73**	E80	D84	E86	H114	**F124**	E127	K131	E145	D148	**I152**	D159	**R179**	W181	**R182**	**R185**	N188
kH_V1	**L48**	**D51**	G58	E62	Y64	E109	**F119**	E122	L126	H140	D143	**V147**	E154	**R174**	W176	**R177**	**R180**	H183
PtH_V1	**L89**	**D92**	E99	L103	Q105	F170	**F180**	E183	T187	Y202	D205	**V209**	E216	**R238**	W240	**R241**	**R244**	H247
CbH_V1	**L111**	**D114**	E121	D125	E127	F200	**F210**	E213	L217	Y232	D235	**V239**	E246	**R268**	W270	**R271**	**R274**	H277
EhH_V1	**L124**	**D127**	E134	D138	E140	T210	**F220**	E223	L227	Y242	D245	**V249**	E256	**R276**	W278	**R279**	**R282**	H285
c15orf27	**V108**	V111	E118	D122	K124	H139	**F149**	E152	R156	E171	D174	**I178**	M185	**R208**	W210	**R211**	**R214**	D217
CiVSP	**I126**	D129	D136	K142	E144	D151	**F161**	D164	R168	E183	D186	**I190**	T197	**R223**	L225	**R226**	**R229**	**R232**
Shaker	**I237**	S240	E247	E251	K253	F280	**F290**	E293	R297	N313	D316	**I320**	A328	**R365**	V367	**R368**	**R371**	**K374**
$K_V1.2$	**I173**	S176	E183	D194	H196	F223	**F233**	E236	R240	N253	D259	**I263**	Y266	**R300**	M302	**R303**	**R306**	**K309**

Species are indicated by one- or two-letter abbreviations: h, human; m, mouse; Ci, *Ciona intestinalis*; Np, *Nicoletia phytophila*; Sp, *Strongylocentrotus purpuratus*; k, *Karlodinium veneficum*; Pt, *Phaeodactylum tricornutum*; Cb, *Coccolithus braarudii*; Eh, *Emiliania huxleyi*. HG, hydrophobic gasket residues (gray); Sel, selectivity filter (yellow). Zn^{2+}, one of the two Zn^{2+}-binding His (in some species). Green-shaded residues sense voltage. Okamura et al. (2015) propose a slightly different hydrophobic plug based on the mH_V1 crystal structure: F146, M147, L150, and F178. Several alignments of the S4 helix have been produced, which result in shifts in the register of the basic residues. Kv1.2 is human, NCBI Reference Sequence accession no. NP_004965.1; Shaker is UniProt/Swiss-Prot accession no. P08510.3.

Numbering for both corresponds to hH_V1, although the closed structure is of mH_V1.

We hope that this assembly of information will in itself allow some general conclusions about structure–function relationships. Most existing data appear reasonably consistent, but in some instances, there appear to be species differences. It is unclear whether these are real or simply examples of laboratory to laboratory variation; such observations are inevitably somewhat anecdotal. We also identify examples of qualitatively different outcomes for the same mutation studied in different expression systems. In addition to listing the outcomes of mutations, the motivation for several strategies for generating mutants is discussed. The mutation studies have resulted in rapid progress in understanding how H_V1 works, but many important questions remain. One word of caution must be stated: mutations are designed to test the effect of changing one or more amino acids, usually with the assumption that the rest of the protein will assemble and function exactly as the WT does. This assumption can be tested rigorously only by determining the structure of every mutant. Although this procedure became almost routine for the bacterial reaction center (Xu et al., 2004), it is not remotely possible for H_V1. Nevertheless, many mutants function with little overt change beyond what might be imagined. On the other hand, mutations that alter charge may have powerful effects on structure and hence function at least locally if not globally.

Data organization and exclusions

The information in this review is organized according to the amino acid numbering of the human voltage-gated proton channel, hH_V1. To make the tables more manageable, we present the mutants in numerical order (with a few exceptions whose logic may or may not become apparent) and include separate tables for the N terminus, for each TM helix (S1–S4), and for the C terminus. The boundaries of the TM helices are defined according to the electron paramagnetic resonance (EPR) study of Li et al. (2015). Double or triple mutants are listed according to the first (i.e., nearest the N terminus) position mutated (again with a few exceptions whose rationale may become apparent). The intention is to make these tables exhaustive as far as is practical, but our bias is toward electrophysiological descriptions of individual point mutants. Thus, we do not list all 109 mutants studied by Cys scanning and assessed for accessibility by PEGylation protection (Sakata et al., 2010; Kurokawa and Okamura, 2014), for example. Nor

Downloaded from http://rupress.org/jgp/article-pdf/148/2/97/1795854/jgp_201611619.pdf by guest on 08 February 2026

Table 2. **Changes in H_V1 properties in N-terminal (1–100) mutants versus WT channels**

Mutant	Species	Expr. system	*I*?	τ_{act}	τ_{tail}	ΔV_{thr}	ΔpH slope	Selectivity	Other	Reference
	hH_V1_S	LK35.2 wc	Yes	2.5	0.75	5.4	43.2	H^+	More profound enhanced gating	Hondares et al., 2014
T9A	hH_V1_S	LK35.2 pp	Yes	0.28	0.9	−18.2			Enhanced gating lost	Hondares et al., 2014
S77A	hH_V1_S	LK35.2 pp	Yes	1.75	1.1	−3.6			nc	Hondares et al., 2014
T9A/S77A	hH_V1_S	LK35.2 pp	Yes	0.63	0.8	−5.8			Enhanced gating lost	Hondares et al., 2014
T29A	hH_V1	LK35.2 pp	Yes	0.23	1.8	−27.6			Enhanced gating lost	Musset et al., 2010a
T29D	hH_V1	LK35.2 pp	Yes	0.41	1.0	−12.5			Enhanced gating lost	Musset et al., 2010a
M91T	hH_V1	COS wc	Yes			20	47		First identified naturally occurring hH_V1 mutation	Iovannisci et al., 2010
S97A	hH_V1	LK35.2 pp	Yes	0.96	1.2	3.9			nc	Musset et al., 2010a
S97D	hH_V1	LK35.2 pp	Yes	0.34	0.9	−3.0			nc	Musset et al., 2010a
T29A/S97A	hH_V1	LK35.2 pp	Yes	0.25	1.7	−19.4			Enhanced gating lost	Musset et al., 2010a
S98A	hH_V1	HEK wc	Yes			−7				Ramsey et al., 2010
H99A	hH_V1	HEK wc	Yes			13				Ramsey et al., 2010
R100A	hH_V1	HEK wc	Yes			−7				Ramsey et al., 2010
ΔN (1–96 deleted)	hH_V1	HEK wc	Yes			15	40			Ramsey et al., 2010
ΔN/ΔC	mH_V1 (1–77 deleted, V216stop)	HEK wc	Yes	0.20		nc	nc		Loss of dimer formation	Koch et al., 2008
ΔN/ΔC	mH_V1 (1–77 deleted, V216stop)	HEK i-o	Yes						Weaker Zn^{2+} effects	Musset et al., 2010b

That numerical entries are shown does not imply that any given change was significant. The entries for hH_V1_S are in a short isoform and are compared with full-length hH_V1. HEK, HEK-293, HEK-293T, tsA, or HM1; COS, COS-7; pp, perforated patch; wc, whole cell; i-o, inside-out patch configuration. Blank entries indicate that the parameter was not examined. nc, measured, but no change. Parameters are given relative to WT in each study. For *I*?, yes means currents are detectable. Time constants are ratios of mutant/WT. The $\Delta V_{threshold}$ value is the change in absolute position of the g_H–*V* relationship versus WT. The ΔpH slope is the slope in millivolts of the relationship between $V_{threshold}$ (or other parameters reflecting the absolute position of the g_H–*V* relationship) and V_{rev} or E_H (which are not identical; see section Table entries defined). When C-terminal truncations (ΔC) are indicated as XNNNstop, this means STOP replaces X at position NNN; hence, position NNN and all subsequent residues are truncated, and the last position remaining is NNN-1. The mouse N-terminal deletions (ΔN) were done by replacing P78M to initiate translation at that position.

do we list all 149 positions at which Cys was introduced for EPR measurements (Li et al., 2015). These blanket mutations are interpretable mainly within the context of the entire study. We exclude most mutations examining the link between S4 and the C terminus, which involve a large variety of deletions and insertions (Fujiwara et al., 2012, 2014). Mutations to the coiled-coil region of the C terminus resulting in trimeric and tetrameric channels (Fujiwara et al., 2013a) are not discussed here. Only a fraction of a large series of Trp scanning mutants in both monomeric and dimeric constructs is listed (Okuda et al., 2016). A series of mutants and tandem constructs in which one or both of the His that bind Zn^{2+} (His^{140} and His^{193}) were replaced (Musset et al., 2010b) is not included in the tables. A series of Cys cross-linking mutations aimed at identifying the dimer interface (Lee et al., 2008) is also omitted. Finally, we do not include domain-swap mutants, such as those of Alabi et al. (2007), in part because chimerae do not logically fit into the format of the tables.

Table entries defined

The first column lists the mutations as per the usual convention (single-letter amino acid abbreviations: WT, position counting from the N terminus, and replacement). When a study used a nonhuman species, the hH_V1 equivalent is given in italics in the first column, and the actual mutation is listed in the second column. The third column gives the expression system and the voltage-clamp method used. To our knowledge, no studies exist in which different properties were observed in HEK versus COS cells (Musset et al., 2008a). However, mammalian versus amphibian studies sometimes differ. For example, D112S from three different species all expressed well and exhibited anion permeation in mammalian cells (Musset et al., 2011; Smith et al., 2011; Chaves et al., 2016), whereas currents were not observed in *Xenopus laevis* oocytes (Berger and Isacoff, 2011). Some proteins function better in certain expression systems: CiH_V1 works well in *Xenopus* oocytes, whereas mH_V1 does not and prefers mammalian (HEK) cells (Okuda et al., 2016). Among mammalian cells, hH_V1 expressed in the B cell–related LK35.2 cell line exhibits an enhanced gating response to stimulation with PMA (Musset et al., 2010a; Hondares et al., 2014), whereas hH_V1 expressed in HEK or COS cells did not respond (Musset et al., 2008a).

The fourth column (*I*?) simply reports whether interpretable currents were observed. A positive answer means the mutant protein is produced, reaches the plasma membrane, and functions. A negative result may have various undetermined explanations (protein

Downloaded from http://rupress.org/jgp/article-pdf/148/2/97/1795854/jgp_201611619.pdf by guest on 08 February 2026

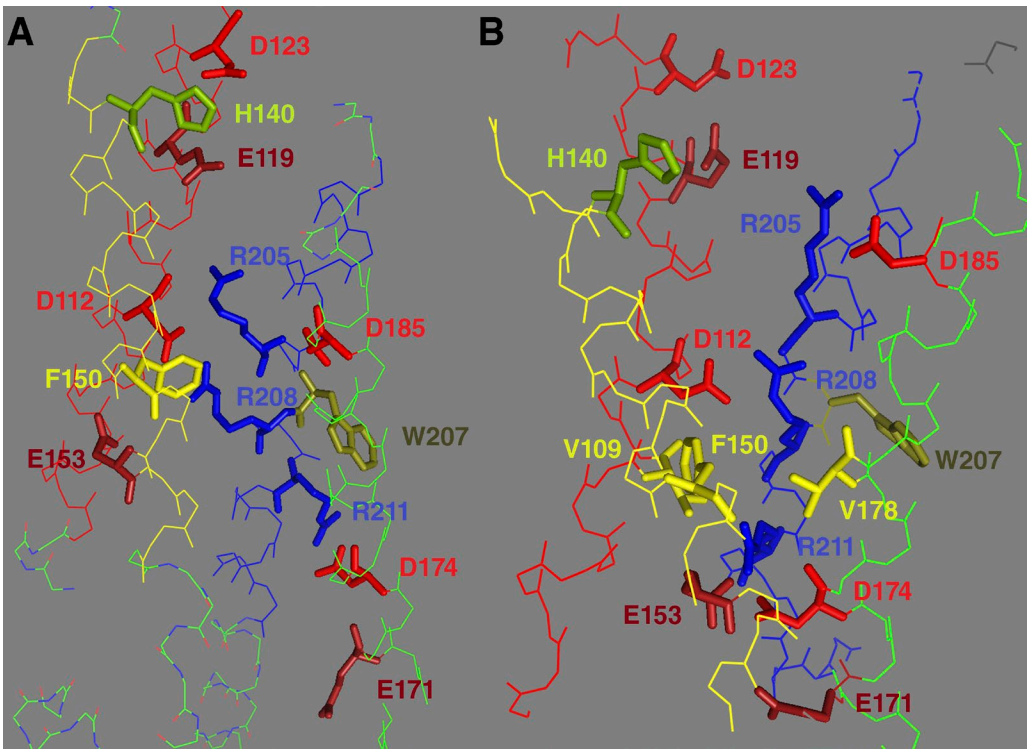

Figure 2. **Location of key amino acids.** Location of some key amino acids in the crystal structure of the mH$_V$1 chimera (Takeshita et al., 2014), labeled with hH$_V$1 numbers (A), and in an open state model of hH$_V$1, R2D (B; Kulleperuma et al., 2013). The channels are viewed from the side with the extracellular end at the top. An EPR study of hH$_V$1 generally agreed with the structure of the mH$_V$1 chimera, except in the EPR study the S2 helix (with F150 and E153) was one turn of the helix lower and S3 (with D174 and D185) was one turn higher relative to S1 and S4 (DeCoursey, 2015a; Li et al., 2015). E153 is the first amino acid replaced by the spliced-in CiVSP segment, and is actually D in the crystal. The images were produced with the PyMOL Molecular Graphics System (version 1.8; Schrödinger, LLC).

misfolding, failure to traffic to the plasma membrane, disruption of gating or permeation) but is nevertheless potentially important because amino acids that play crucial roles in function may be difficult to replace without disrupting molecular function. For example, Asp^{112} and Arg^{208} form a crucial nexus that in general cannot be meddled with without altering or eliminating function. However, different laboratories may have different criteria for deciding whether small currents are "real," small enough to be negligible, or nonexistent. This evaluation is complicated by the fact that all common mammalian expression systems (HEK, Chinese hamster ovary [CHO], and COS cells) frequently display (typically small) native voltage-gated proton currents (Cherny et al., 1997; Musset et al., 2011). To address this concern, we often introduce mutations into hH$_V$1 in a Zn^{2+}-insensitive background, meaning the two His primarily responsible for Zn^{2+} inhibition are mutated (H140A/H193A; Ramsey et al., 2006; Musset et al., 2010b). Then, if we see small currents that might be due either to native currents or to expression of a poorly conducting mutant, we add 10 µM Zn^{2+}, which profoundly inhibits WT hH$_V$1, but will have negligible effects on a Zn^{2+}-insensitive mutant. This approach cannot be applied to H$_V$1 from species lacking these His (Table 1).

The gating kinetics columns are self-evident: τ_{act} is the activation (channel opening) time constant, and τ_{tail} is the tail current or deactivation (channel closing) time constant. These are expressed as the ratio τ_{mutant}/τ_{WT} so that 1 means no change, a ratio <1 means faster than WT, and a ratio >1 means slower than WT. Because H$_V$1 gating kinetics depends very strongly on temperature, with Q_{10} 6–9 (DeCoursey and Cherny, 1998; Kuno et al., 2009), and is also influenced profoundly by experimental artifacts including proton depletion-induced current decay ("droop") and pH changes, anything less than a twofold change should be viewed with skepticism.

The columns labeled $\Delta V_{threshold}$ (ΔV_{thr}) and ΔpH slope embody one of the crucial and unique properties of this channel, namely its ΔpH-dependent gating. Decreasing pH_i or increasing pH_o shifts the g_H–V relationship negatively by roughly 40 mV/U of change in pH, as originally described by Cherny et al. (1995):

$$V_{threshold} = 20 - 40\Delta pH \quad (1)$$

Downloaded from http://rupress.org/jgp/article-pdf/148/2/97/1795854/jgp_201611619.pdf by guest on 08 February 2026

or, generalized:

$$V_{threshold} = V_0 - V_{slope}\,\Delta pH, \quad (2)$$

where $V_{threshold}$ is the most negative voltage at which detectable current can be elicited, V_0 is $V_{threshold}$ at symmetrical pH (roughly 20 mV), V_{slope} is the steepness (in millivolts/unit pH) of the relationship (nominally 40 mV), and $\Delta pH = pH_o - pH_i$. The precise value for V_{slope} depends on whether the abscissae are E_H (the Nernst potential for H^+ based on the nominal pH of the solutions) or the measured V_{rev}. Because V_{rev} often changes by less than a Nernstian amount in real experiments (almost certainly as a result of our inability to perfectly control pH, in combination with pH changes due to the measurement itself), plotting $V_{threshold}$ against the measured V_{rev} usually produces a larger slope. Thus, the shift of $V_{threshold}$ (vs. V_{rev}) for native proton currents measured in rat alveolar epithelial cells was 44 mV/U (Cherny et al., 1995). The mean shift reported in 15 types of cells was 46 mV/U (DeCoursey, 2003b). The slope for hH_V1 transfected into HEK or COS cells was 39–43 mV/U (Musset et al., 2008a). There are essentially no reports of mutants in which V_{slope} departs convincingly from this range. Two nominal deviations from this rule are R211A (53 mV) and ΔN (28 mV; Ramsey et al., 2010), but their P-values versus WT are 0.04 and 0.02, and 2/31 values in this study could easily fall just under the arbitrary P = 0.05 cutoff by chance.

Rather than give an absolute value for the position of the g_H–V relationship, such as using the parameter V_0 in Eq. 2 above (which is not in common parlance), we list the change of $V_{threshold}$ (V_{thr}) or an equivalent parameter from control values in each study. Actual numbers will depend on conventions in each laboratory. When data were reported for asymmetrical pH, the $V_{threshold}$ value was "corrected" by shifting it by 40 mV/U change in ΔpH (Cherny et al., 1995). For reasons discussed at length elsewhere (Musset et al., 2008a), we consider it a highly questionable practice to fit whole-cell g_H–V data with a Boltzmann function, as is routinely done for other voltage-gated channels. Because the distortion of current amplitudes and kinetics resulting from proton depletion are ubiquitous and profound, we prefer to quantify absolute voltage dependence by $V_{threshold}$ (the most negative voltage at which discernable time-dependent H^+ currents are detected) or $V_{gH,max/10}$ (the voltage at which the g_H is 10% of its maximal value), both measured during small depolarizations and thus minimizing depletion. The absolute position of the g_H–V relationship appears quite mutable with mutation; the extensive study of Ramsey et al. (2010) produced examples spanning >200 mV for various mutants. Given the technical difficulty and intrinsic variability of $V_{threshold}$ estimation, it would be dangerous to draw conclusions about shifts of less than ∼20 mV. There is a 30-mV range of values reported for WT hH_V1 (see Table 3 in DeCoursey, 2013).

Selectivity is given only when it was explicitly evaluated. The WT channel is perfectly selective for protons, so H^+ is entered. The entry Cl^- means that the channel is permeable to Cl^- and likely to other anions as well; Na^+ means the channel is permeable to Na^+ and likely other cations besides H^+. The column Other simply provides concise information that does not fit elsewhere in the tables.

Table 2: The N terminus (positions 1–100 in hH_V1)

N terminus. The N terminus of hH_V1 comprises 100 amino acids and is intracellular. The effects of truncating the entire N terminus (ΔN) are not dramatic. Deleting both the N and C termini (ΔN/ΔC) simultaneously results in five- to sixfold faster activation, presumably because these truncations result in monomeric constructs. Although coiled-coil interactions in the C terminus are generally considered to be the main interaction that stabilizes the dimer (Koch et al., 2008; Lee et al., 2008; Tombola et al., 2008; Fujiwara et al., 2013b, 2014; Smith and DeCoursey, 2013), deleting both N and C termini (ΔN/ΔC) appeared to produce monomers more reliably (Koch et al., 2008). Nevertheless, even when both N and C termini are deleted, the VSD-only construct spontaneously dimerizes with a K_d of ∼3 µM (Li et al., 2015).

The short isoform, hH_V1_S. Some B cells, especially B lymphocytes from chronic lymphocytic leukemia patients or malignant B cell lines (Hondares et al., 2014), express a short isoform of hH_V1 (hH_V1_S) that lacks the first 20 amino acids (Capasso et al., 2010). Fig. 1 shows that the 21st amino acid is Met (ATG), which acts as an alternative start site (Hondares et al., 2014). Compared with the full-length protein, hH_V1_S opens more slowly, and its enhanced gating response to PMA is more profound. Furthermore, hH_V1_S interacts less with the B cell receptor, resulting in less internalization. Together, its properties suggest that its expression may contribute to the pathogenesis of B cell malignancies (Hondares et al., 2014).

The phosphorylation site responsible for enhanced gating. When phagocytes are stimulated to undergo the respiratory burst (i.e., activation of NADPH oxidase, or NOX2), the properties of proton channels change so dramatically (Bánfi et al., 1999; DeCoursey et al., 2000; Musset et al., 2009) that at first, the appearance of a second, distinct type of proton channel (proposed to be a component of the active NADPH oxidase complex) was hypothesized (Henderson et al., 1995; Henderson and Chappell, 1996; Bánfi et al., 1999). A decade of controversy ensued (Henderson et al., 1997; Henderson, 1998; Henderson and Meech, 1999, 2002; De-

Downloaded from http://rupress.org/jgp/article-pdf/148/2/97/1795854/jgp_201611619.pdf by guest on 08 February 2026

Coursey et al., 2001b, 2002, 2003; Maturana et al., 2002; Touret and Grinstein, 2002; DeCoursey, 2003a,b, 2016). The idea that the gp91^{phox} component of NADPH oxidase could function as a proton channel was not dispelled completely until well after the HVCN1 gene was identified (Ramsey et al., 2006; Sasaki et al., 2006) when the HVCN1 knockout mouse was developed, which provided the final nail in the coffin (Morgan et al., 2009; El Chemaly et al., 2010). In activated phagocytes, four characteristics of H^+ currents change, all in the direction of increasing proton flux: the maximum g_H increases two- to fourfold, the g_H–V relationship shifts negatively by 30–40 mV, τ_{act} becomes two to five times faster, and τ_{tail} slows two- to sixfold (DeCoursey et al., 2000, 2001a,b; Cherny et al., 2001; DeCoursey, 2003a; Musset et al., 2009). This is referred to as the enhanced gating mode to emphasize that the properties of the H_V1 channel change as a result of phosphorylation, as opposed to a second type of channel appearing.

The original mechanism proposed for enhanced gating of H_V1 was not phosphorylation, but rather modulation of the channel by arachidonic acid generated by cPLA$_2\alpha$ (Henderson and Chappell, 1992). Although arachidonic acid does enhance H_V1 gating by a direct pharmacological effect (DeCoursey and Cherny, 1993; Kapus et al., 1994; Suszták et al., 1997; Kawanabe and Okamura, 2016), neither specific cPLA$_2\alpha$ inhibition nor genetic knockout of cPLA$_2\alpha$ affects the activation of NADPH oxidase or the enhanced gating of H_V1 channels during the respiratory burst (Morgan et al., 2007).

Two predicted PKC phosphorylation sites, Thr^{29} and Ser^{97}, were studied in hH_V1 expressed in the B cell–related LK35.2 cell line (Musset et al., 2010a). Although both were detectably phosphorylated, mutation of Thr^{29} but not Ser^{97} abolished the enhanced gating response, implicating Thr^{29} as the key PKC phosphorylation site in hH_V1 (Musset et al., 2010a). Analogous studies of the short isoform identified the same residue, Thr^9, as the main phosphorylation site (Hondares et al., 2014).

The first identified human hH_V1 mutation. The first naturally occurring hH_V1 mutation from a human subject, M91T (Table 2), was identified by Iovannisci et al. (2010), who cloned *HVCN1* genes from primary human airway tissue cultures. Unfortunately, the mutation was discovered only after the death of the donor, who consequently had no opportunity to mourn the defective nature of his/her proton channels, and we lack the opportunity to evaluate the effects of the mutation on his/her quality of life. The main effect of the mutation on H_V1 expressed in COS cells is to decrease the likelihood of channel opening. It requires ~20 mV more depolarization or ~0.5 U of greater ΔpH (for airway epithelia, this likely means a higher pH_o) to open mutant M91T channels (Iovannisci et al., 2010).

Table 3: The S1 helix (positions 101–125) and the S1–S2 linker (126–133)

The selectivity filter, Asp^{112}. The most intensively studied position in hH_V1 is Asp^{112}, which was implicated in proton flux (Letts, 2014) and was identified as a crucial part of the selectivity filter (Musset et al., 2011). An indication of the importance of this position is that most mutants malfunction or fail to function altogether, although with some unexplained apparent variability between species or expression systems. Mutation of Asp^{112} to a neutral residue in most cases results in anion conduction. Specifically, replacing the large anion methanesulfonate$^-$ in the external solution with the smaller Cl^- shifts V_{rev} negatively, demonstrating permeability to Cl^- (Musset et al., 2011). Lowering the ionic strength by 90% shifts V_{rev} positively, confirming anion over cation permeation (Musset et al., 2011). Quite similar phenomenology supports an identical role for the analogous Asp in the middle of the S1 helix in two evolutionarily distant species, *Karlodinium veneficum* (Smith et al., 2011) and *Nicoletia phytophila* (Chaves et al., 2016), which respectively are only 15% and 33% identical to hH_V1. The conductance of Asp^{112} mutants appears to vary inversely with the hydrophobicity of the substituent at position 112, with two of the most hydrophobic amino acids tested, Val and Ile, eliminating current flow altogether (Musset et al., 2011; DeCoursey, 2015b). The conservative Asp→Glu mutant retains proton selectivity.

Clearly, Asp^{112} is crucial to the proton selectivity of hH_V1. However, other Asp are present in the presumed conduction pathway, such as Asp^{185} (Fig. 2), but Table 5 shows that its mutation does not impair H^+ flux (Letts, 2014) or H^+ selectivity (Musset et al., 2011). In an attempt to determine what other requirements exist for selectivity, Asp was moved along the S1 helix to each position from 108 to 118 (Morgan et al., 2013). At most positions where Asp faced away from the pore, no current was observed. Asp produced proton selectivity at just one other position, 116. Molecular dynamics (MD) simulations suggest that the D112V/V116D construct is proton selective only when Asp^{116} interacts with one or more S4 Arg residues (Morgan et al., 2013). This result shows that not every near-neighbor interaction of Asp^{112} in its native position is necessary, but there are clearly strong constraints. The requirements for proton selectivity in hH_V1 deduced from these and many other mutations include the following: (a) a carboxyl group (Asp or Glu) is required; (b) it must face the pore; (c) it must be located at a narrow point in the channel; and (d) it must be able to interact with a basic group (Arg or Lys).

These conditions apparently exist only in the outer vestibule of hH_V1. Furthermore, several attempts to reposition Asp into S2 or S3 failed to produce a proton-se-

Downloaded from http://rupress.org/jgp/article-pdf/148/2/97/1795854/jgp_201611619.pdf by guest on 08 February 2026

Table 3. **Changes in H_V1 properties in S1 (101–125) and S1–S2 linker (126–133) mutants versus WT channels**

Mutant	Species	Expr. system	I_t^2	τ_{act}	τ_{tail}	ΔV_{thr}	ΔpH slope	Selectivity	Other	Reference
Q102C	CiH_V1 [H150C]	*Xenopus* i-o	Yes						MTS_i access	Mony et al., 2015
V103C	CiH_V1 [V151C]	*Xenopus* i-o	Yes						MTS_i open> closed	Mony et al., 2015
I105C	CiH_V1 [I153C]	*Xenopus* i-o	Yes						MTS_i open> closed	Mony et al., 2015
I106C	CiH_V1 [I154C]	*Xenopus* i-o	Yes						MTS_i open> closed	Mony et al., 2015
C107A	hH_V1	HEK wc	Yes			−17				Ramsey et al., 2010
C107S	hH_V1								90% dimer	Li et al., 2015
V109C	CiH_V1 [V157C]	*Xenopus* i-o	Yes						MTS_i open> closed	Mony et al., 2015
V109A	hH_V1	*Xenopus* i-o	Yes			−11				Hong et al., 2014
D112A	hH_V1	HEK wc	Yes			59	38			Ramsey et al., 2010
D112A[a]	hH_V1	COS/HEK wc	Yes	2.2	3.0	41[b]	43	Cl^-		Musset et al., 2011
D112A	hH_V1	Vesicle flux							Slows H^+ flux	Letts, 2014
D112A	hH_V1	*Xenopus* i-o	No							Hong et al., 2014
D112A	CiH_V1 [D160A]	*Xenopus* TEVC	No							Chamberlin et al., 2015
D112A	kH_V1 [D51A]	COS/HEK wc	Yes					Cl^-		Smith et al., 2011
D112A	NpHv1 [D66A]	HEK wc	Yes					Cl^-		Chaves et al., 2016
D112C	CiH_V1 [D160C]	*Xenopus* TEVC	No							Chamberlin et al., 2015
D112C	NpHv1 [D66C]	HEK wc	No							Chaves et al., 2016
D112C/R211C	CiH_V1 [D160C/ R261C]	*Xenopus* TEVC	Yes				nc	Na^+		Chamberlin et al., 2015
D112N	hH_V1	HEK wc	Yes			31	42			Ramsey et al., 2010
D112N[a]	hH_V1	COS/HEK wc	Yes	2.4	3.0	23[b]	35	Cl^-		Musset et al., 2011
D112N/D185A	hH_V1	HEK wc	Yes			103				Ramsey et al., 2010
D112A	hH_V1	*Xenopus* i-o	No							Hong et al., 2014
D112E	hH_V1	*Xenopus* i-o	Yes			−13				Hong et al., 2014
D112E	hH_V1	COS/HEK wc	Yes	0.18	7.4/.085	−11[b]	34	H^+	Biexponential tails	Musset et al., 2011
D112E	hH_V1	*Xenopus* i-o	Yes			−15				Berger and Isacoff, 2011
D112E	kH_V1 [D51E]	COS/HEK wc	Yes					H^+		Smith et al., 2011
D112E	NpHv1 [D66E]	HEK wc	Yes					H^+		Chaves et al., 2016
D112E/I127C	CiH_V1 [D160A/ I175C]	*Xenopus* i-o	Yes	nc	4.0					Mony et al., 2015
D112H	hH_V1	COS/HEK wc	Yes	2.0	0.85	13[b]	38	Cl^-		Musset et al., 2011
D112H	kH_V1 [D51H]	COS/HEK wc	Yes					Cl^-		Smith et al., 2011
D112H	NpHv1 [D66H]	HEK wc	Yes					Cl^-		Chaves et al., 2016
D112K[a]	hH_V1	COS/HEK wc	Yes	0.8	0.22	46[b]	40	Cl^-		Musset et al., 2011
D112S	hH_V1	COS/HEK wc	Yes	2.0	4.1	25[b]	38	Cl^-		Musset et al., 2011
D112S	hH_V1	*Xenopus* i-o	No							Berger and Isacoff, 2011
D112S	hH_V1	Vesicle flux							Slows H^+ flux	Letts, 2014
D112S	kH_V1 [D51S]	COS/HEK wc	Yes					Cl^-		Smith et al., 2011
D112S	NpHv1 [D66S]	HEK wc	Yes					Cl^-		Chaves et al., 2016
D112S/R211S	hH_V1	*Xenopus* i-o	Yes			24	44	Gu^+	At pH 8//8	Berger and Isacoff, 2011
D112F[a]	hH_V1	COS/HEK wc	Yes	1.6	0.03	44[b]	38	Cl^-		Musset et al., 2011
D112R/R211D	hH_V1	*Xenopus* i-o	Yes					H^+		Berger and Isacoff, 2011
D112V	hH_V1	COS/HEK wc	No							Musset et al., 2011
D112L	hH_V1	Vesicle flux							Slows H^+ flux	Letts, 2014
D112I[a]	hH_V1	COS/HEK wc	No							DeCoursey, 2015b
D112Q	hH_V1	*Xenopus* i-o	No							Hong et al., 2014
D112A/L108D[a]	hH_V1	COS/HEK wc	No							Morgan et al., 2013
D112V/V109D[a]	hH_V1	COS/HEK wc	No							Morgan et al., 2013
D112A/V109D[a]	hH_V1	COS/HEK wc	Yes					Cl^-		Morgan et al., 2013
D112A/V110D[a]	hH_V1	COS/HEK wc	No							Morgan et al., 2013
D112A/L111D[a]	hH_V1	COS/HEK wc	No							Morgan et al., 2013
D112A/A113D[a]	hH_V1	COS/HEK wc	No							Morgan et al., 2013
D112A/L114D[a]	hH_V1	COS/HEK wc	No							Morgan et al., 2013
D112A/L115D[a]	hH_V1	COS/HEK wc	No							Morgan et al., 2013
D112A/V116D[a]	hH_V1	COS/HEK wc	Yes					H^+		Morgan et al., 2013
D112V/V116D[a]	hH_V1	COS/HEK wc	Yes					H^+		Morgan et al., 2013
D112V/V116E[a]	hH_V1	COS/HEK wc	Yes					H^+		Morgan et al., 2013
D112V/V116S[a]	hH_V1	COS/HEK wc	Yes					Cl^-		Morgan et al., 2013
D112V/V116N[a]	hH_V1	COS/HEK wc	Yes					Cl^-		Morgan et al., 2013
D112A/L117D[a]	hH_V1	COS/HEK wc	No							Morgan et al., 2013
D112A/A118D[a]	hH_V1	COS/HEK wc	No							Morgan et al., 2013
D112N/I127C	CiH_V1 [D160N/I175C]	*Xenopus* i-o	No							Mony et al., 2015
D112N/ R211S/I127C	CiH_V1 [D160N/ R261S/I175C]	*Xenopus* i-o	Yes			15				Mony et al., 2015

Downloaded from http://rupress.org/jgp/article-pdf/148/2/97/1795854/jgp_201611619.pdf by guest on 08 February 2026

Table 3. **Changes in H_V1 properties in S1 (101–125) and S1–S2 linker (126–133) mutants versus WT channels** *(Continued)*

Mutant	Species	Expr. system	$I_H^?$	τ_{act}	τ_{tail}	ΔV_{thr}	ΔpH slope	Selectivity	Other	Reference
D112N/R211S/G199C	CiH_V1 [D160N/R261S/G249C]	*Xenopus* i-o	Yes			44				Mony et al., 2015
D112N/G199C	CiH_V1 [D160N/G249C]	*Xenopus* i-o	No							Mony et al., 2015
A113D[a]	hH_V1	COS/HEK wc	Yes					H^+		Morgan et al., 2013
E119A	hH_V1	HEK wc	Yes			20	47			Ramsey et al., 2010
E119L	hH_V1	Vesicle flux							nc H^+ flux	Letts, 2014
E119S	mH_V1 [E115S]	HEK wc	Yes						nc Zn^{2+} inhibition	Takeshita et al., 2014
E119S/D123S	mH_V1 [E115S/D119S]	HEK wc	Yes						Weaker Zn^{2+} inhibition	Takeshita et al., 2014
E119A	CiH_V1 [E167A]	*Xenopus* TEVC	Yes			4				Chamberlin et al., 2014
E119C/R205C	CiH_V1 [E167C/R255C]	*Xenopus* TEVC	Yes			−2				Chamberlin et al., 2014
E119C/R208	CiH_V1 [E167C/R258C]	*Xenopus* TEVC	Yes			−52				Chamberlin et al., 2014
D123A	hH_V1	HEK wc	Yes			20	48			Ramsey et al., 2010
D123S	mH_V1 [D119S]	HEK wc	Yes						nc Zn^{2+} inhibition	Takeshita et al., 2014
D123C	CiH_V1 [D171C]	*Xenopus* i-o	Yes						MTS_o open> closed	Mony et al., 2015
D123A	CiH_V1 [D171A]	*Xenopus* TEVC	Yes			72				Chamberlin et al., 2014
D123A/R205N	CiH_V1 [D171A/R255N]	*Xenopus* TEVC	Yes			11				Chamberlin et al., 2014
K125A	hH_V1	HEK wc	Yes			19	47			Ramsey et al., 2010
K125C	CiH_V1 [K173C]	*Xenopus* i-o	Yes						MTS_o access	Mony et al., 2015
I127C	CiH_V1 [I175C]	*Xenopus* i-o	Yes			0				Mony et al., 2015
D130A	hH_V1	HEK wc	Yes			13				Ramsey et al., 2010
K131A	hH_V1	HEK wc	Yes			33				Ramsey et al., 2010

That numerical entries are shown does not imply that any given change was significant. Italicized mutant entries from nonhuman species show the hH_V1 equivalent. HEK, HEK-293, HEK-293T, tsA, or HM1; COS, COS-7; *Xenopus*, *Xenopus laevis* oocyte; wc, whole cell; i-o, inside-out patch configuration; TEVC, two-electrode voltage clamp. Blank entries indicate that the parameter was not examined. nc, measured, but no change. Parameters are given relative to WT in each study. For $I_H^?$, yes means currents are detectable. Time constants are ratios of mutant/WT. The $\Delta V_{threshold}$ value is the change in absolute position of the g_H–V relationship versus WT. The ΔpH slope is the slope in millivolts of the relationship between $V_{threshold}$ (or other parameters reflecting the absolute position of the g_H–V relationship) and V_{rev} or E_H (which are not identical; see section Table entries defined). For column Other, MTS access from inside or outside (MTS_i or MTS_o, respectively) is listed as open>closed if the open channel was more accessible.

[a]In an H140A/H193A (Zn^{2+} insensitive) background.

[b]Previously unpublished, analyzed from data for Musset et al. (2011).

lective conductance, suggesting that, for reasons that are not at all clear, the carboxyl group must be on S1. A quantum model of the selectivity filter of hH_V1 illustrates how interacting Asp and Arg side chains can selectively conduct protons while excluding other ions (Dudev et al., 2015).

Intriguingly, proton-selective conduction is preserved when Asp^{112} is replaced by Glu^{112} (Musset et al., 2011) or when Arg^{208} is replaced by Lys^{208} (Dudev et al., 2015). Clearly, this critical interaction has leeway with respect to chain length. The F_1F_o ATP synthase (H^+ translocating ATPase) remarkably parallels H_V1 in that the proton pathway in its *c* subunit has an essential Asp^{61}–Arg^{210} pair and Asp^{61} can be moved to a different location or replaced by Glu with only partial loss of function (Miller et al., 1990). It is noteworthy that in several other molecules with critical proton transport pathways, analogous substitutions impair function: Asp→Glu (Chen et al., 2000; Ruivo et al., 2012; Luoto et al., 2013), Glu→Asp (Thorndycroft et al., 2007; Cornish et al., 2011), and Lys→Arg (Balashov et al., 2013). Li et al. (2015) found that hH_V1 is more mobile and dynamic than VSDs of other voltage-gated ion channels.

The series of mutations to Asp^{112} nicely illustrates the difficulty of interpreting mutations. For example, D112A, D112S, and D112N (Table 3) all open and close more slowly than WT. So is the function of Asp^{112} to speed gating? No, because D112K produced faster kinetics, and D112F changed activation and deactivation in opposite directions. So does Asp^{112} regulate gating kinetics? Not really, because practically every mutation for which kinetics were reported alters kinetics, by up to 100-fold. Considering that gating reflects large conformational changes and perhaps other subtler changes that involve a large fraction of the amino acids in the protein, and H_V1 is a compact molecule, it is not surprising that most mutations affect gating kinetics. Their interpretation requires semantic judiciousness. Not every position whose mutation affects gating can reasonably be said to regulate gating kinetics. Nevertheless, the effects of mutations are real and suggest involvement in the process, whose mechanism may, however, be difficult to disentangle.

Countercharges in S1. A fundamental principle in the conception of how voltage gating works is that the peri-

Downloaded from http://rupress.org/jgp/article-pdf/148/2/97/1795854/jgp_201611619.pdf by guest on 08 February 2026

odically spaced cationic residues in S4 (Arg and sometimes Lys) that sense voltage interact electrostatically with anionic amino acids elsewhere in the channel protein to stabilize both closed and open states (Papazian et al., 1995; Tiwari-Woodruff et al., 1997; Lecar et al., 2003). In the General conclusions section below, we discuss alternative interpretations. Within the charge/countercharge conceptual framework, externally accessible acidic residues stabilize the open state, and internally accessible acidic groups stabilize the closed state, presumably by interacting with the cationic groups in S4. If this is the case, a neutralizing mutation to such an externally accessible amino acid should shift the g_H–V relationship positively because the mutant will lose open state stabilization. Conversely, an internal acidic residue would normally stabilize the closed state, and its mutation should promote channel opening, thus shifting the g_H–V relationship negatively. By these criteria, three acidic amino acids in S1 in the outer vestibule, Asp^{112}, Glu^{119}, and Asp^{123}, and possibly Lys^{125} may be considered weak stabilizers of the open state because their neutralization by mutation produces modest positive shifts. Both Asp^{112} and Glu^{119} interact with S4 Arg residues in MD simulations of open state homology models of hH_V1 (Wood et al., 2012; Kulleperuma et al., 2013) and CiH_V1 (Chamberlin et al., 2014).

Table 4: The S2 helix (positions 134–156) and the S2–S3 linker (157–165)

The Zn^{2+}-binding site. The most potent inhibitor of voltage-gated proton currents is Zn^{2+} (Mahaut-Smith, 1989; DeCoursey, 2003b). Unlike traditional channel blockers that occlude the pore, Zn^{2+} shifts the g_H–V relationship positively and slows activation (Cherny and DeCoursey, 1999). These effects were strongly inhibited at low pH_o, indicating competition between Zn^{2+} and H^+ for a binding site. To model the competition between H^+ and Zn^{2+} quantitatively required assuming that Zn^{2+} prevents channel opening by binding to an externally accessible site on the closed channel comprising at least two titratable groups with a pK_a of 6.2–6.6 (near that of His; Cherny and DeCoursey, 1999). Seven years later, the identification of the hH_V1 gene confirmed this deduction because two His residues, His^{140} in S2 and His^{193} in the S3–S4 linker, were found to comprise the main sites at which Zn^{2+} binds to inhibit proton currents (Ramsey et al., 2006). The single mutants H140A and H193A each have diminished sensitivity to Zn^{2+}, and the double mutant is nearly impervious. The Zn^{2+} sensitivity of a series of mutants in which one or both of these His were mutated to Ala, including various tandem dimers, is described elsewhere (Musset et al., 2010b) and is not included in the tables. Remarkably, the crystal structure of the closed mH_V1 channel contained a Zn^{2+} atom tetrahedrally coordinated by the corresponding two His in the mouse (His^{136} and His^{189} in mH_V1), with weaker binding to Glu^{115} and Asp^{119} (Glu^{119} and Asp^{123} in hH_V1).

Countercharges in S2. S2 contains an important countercharge, Glu^{153}, which, as seen in Table 1, is highly conserved among VSD-containing molecules (Smith et al., 2011). In neutral mutants, $V_{threshold}$ is shifted consistently negatively, in some cases by >100 mV, suggesting that this internal acidic residue stabilizes the closed state.

Charge transfer center or hydrophobic gasket. The S2 helix contains Phe^{150}, another highly conserved residue among VSD-containing molecules (Tao et al., 2010; Smith et al., 2011) whose K^+ channel correlate was described as the outer limit of the charge transfer center (Tao et al., 2010). As the positively charged Arg residues in S4 move outwards during a depolarization that opens the channel, they move past Phe^{150}, which serves as a delimiter of internal and external accessibility. Bezanilla and colleagues include Phe^{150} along with two other hydrophobic residues, Val^{109} and Val^{178}, in a hydrophobic gasket (or "plug") that functions similarly (labeled HG in Table 1; Lacroix et al., 2014; Li et al., 2014, 2015; DeCoursey, 2015a). The global purpose of having a narrow isthmus of protein between the two aqueous vestibules is to focus the electric field (Yang et al., 1996, 1997; Starace and Bezanilla, 2001, 2004). This means that each gating charge (e.g., Arg) needs to move only a small distance to effectively cross the entire membrane electrical field. Mutations to Phe^{150} in hH_V1, like those of the corresponding Phe in K^+ channels, shift the g_H–V relationship (Tao et al., 2010; Hong et al., 2013).

Table 5: The S3 helix (positions 166–188) and the S3–S4 linker (189–196)

Countercharges in S3. S3 contains two important countercharges. Asp^{174} is internally accessible and stabilizes the closed state, and neutral mutants shift the g_H–V relationship strongly negatively. In the closed structure of mH_V1, the Asp^{174} equivalent appears to interact with Arg^{211} in an internal pocket (Takeshita et al., 2014; Cherny et al., 2015). Conversely, Asp^{185} (which Table 1 shows is unique to the H_V1 family) is externally accessible and stabilizes the open state, and neutral mutants shift the g_H–V relationship positively. The milder effect of the Asp^{185} mutation mirrors its moderate interaction with Arg^{205} observed in MD simulations of an open state model of hH_V1 (Kulleperuma et al., 2013) and with all three Arg in a model of CiH_V1 (Chamberlin et al., 2014).

Table 6: The S4 helix (positions 197–218)

Cys scanning reveals aqueous accessibility. A now standard approach to demonstrate aqueous accessibility of amino acids in a protein is to convert the target to Cys

Downloaded from http://rupress.org/jgp/article-pdf/148/2/97/1795854/jgp_201611619.pdf by guest on 08 February 2026

Table 4. **Changes in H_V1 properties in S2 (134–156) and S2–S3 linker (157–165) mutants versus WT channels**

Mutant	Species	Expr. system	*I?*	τ_{act}	τ_{tail}	ΔV_{thr}	ΔpH slope	Selectivity	Other	Reference
Y134A	hH_V1	HEK wc	Yes			3				Ramsey et al., 2010
H140A	hH_V1	HEK wc	Yes					H^+	$9 \times K_d$[a] Zn^{2+}	Ramsey et al., 2006
H140A	hH_V1	Vesicle flux							nc H^+ flux	Letts, 2014
H193A	hH_V1	HEK wc	Yes					H^+	$39 \times K_d$[a] Zn^{2+}	Ramsey et al., 2006
H140A/ H193A	hH_V1	HEK wc	Yes			−12	46	H^+	$2{,}000 \times K_d$[a] Zn^{2+}	Ramsey et al., 2006
H140A/ H193A	hH_V1	COS/HEK wc	Yes					H^+		Musset et al., 2011
Y141A	hH_V1	HEK wc	Yes			−27				Ramsey et al., 2010
S143A	hH_V1	HEK wc	Yes			11	41			Ramsey et al., 2010
S143A	hH_V1	Vesicle flux							nc H^+ flux	Letts, 2014
D112V/S143D	hH_V1	COS/HEK wc	Yes					Cl^-		Morgan et al., 2013
D112V/I146D	hH_V1	COS/HEK wc	No							Morgan et al., 2013
D112V/L147D	hH_V1	COS/HEK wc	No							Morgan et al., 2013
F150A	hH_V1	*Xenopus* i-o	Yes			−24				Hong et al., 2013
F150C	hH_V1	*Xenopus* i-o	Yes			−22				Hong et al., 2013
F150W	hH_V1	*Xenopus* i-o	Yes			−55				Hong et al., 2013
E153A	hH_V1	HEK wc	Yes			−55	42			Ramsey et al., 2010
E153A	CiH_V1 [E201A]	*Xenopus* TEVC	No							Chamberlin et al., 2014
E153G	CiH_V1 [E201G]	*Xenopus* TEVC	No							Chamberlin et al., 2014
E153N	hH_V1	HEK wc	Yes			−1.17	45			Ramsey et al., 2010
E153A	hH_V1	Vesicle flux							nc H^+ flux	Letts, 2014
E153D	hH_V1	HEK wc	Yes			−23	37			Ramsey et al., 2010
E153D/D174E	hH_V1	HEK wc	Yes			−102	40			Ramsey et al., 2010
E153C	hH_V1	*Xenopus* i-o	Yes			−55				Tombola et al., 2010
E153C	CiH_V1 [E201C]	*Xenopus* TEVC	Yes			−101				Chamberlin et al., 2014
E153C/R205C	CiH_V1 [E201C/ R255C]	*Xenopus* TEVC	Yes			−43				Chamberlin et al., 2014
E153C/R208	CiH_V1 [E201C/ R258C]	*Xenopus* TEVC	Yes			37				Chamberlin et al., 2014
E153C/R211C	CiH_V1 [E201CR261C]	*Xenopus* TEVC	Yes			−60				Chamberlin et al., 2014
K157A	hH_V1	HEK wc	Yes			1	39			Ramsey et al., 2010
K157A	hH_V1	Vesicle flux							nc H^+ flux	Letts, 2014
R162A	hH_V1	HEK wc	Yes			13				Ramsey et al., 2010

That numerical entries are shown does not imply that any given change was significant. Italicized mutant entries from nonhuman species show the hH_V1 equivalent. HEK, HEK-293, HEK-293T, tsA, or HM1; COS, COS-7; *Xenopus*, *Xenopus laevis* oocyte; wc, whole cell; i-o, inside-out patch configuration; TEVC, two-electrode voltage clamp. Blank entries indicate that the parameter was not examined. nc, measured, but no change. Parameters are given relative to WT in each study. For *I?*, yes means currents are detectable. The $\Delta V_{threshold}$ value is the change in absolute position of the g_H–V relationship versus WT. The ΔpH slope is the slope in millivolts of the relationship between $V_{threshold}$ (or other parameters reflecting the absolute position of the g_H–V relationship) and V_{rev} or E_H (which are not identical; see section Table entries defined).

[a]Nominal K_d values are nearly meaningless for Zn^{2+} inhibition of H_V1 because its main effects are slowing activation and shifting the g_H–V relationship positively (Cherny and DeCoursey, 1999). As demonstrated in the Appendix of DeCoursey et al. (2001a), the apparent K_d derived from the ratio $I_H(Zn^{2+})/I_H$ can vary more than three orders of magnitude depending on the test potential selected. If all measurements are done the same way, relative K_d values have meaning.

and then challenge the mutant with MTS reagents that react with Cys sulfhydryl groups. Whatever functional effect this reaction produces can be examined as a function of the time of exposure to determine accessibility of the Cys. Gonzalez et al. (2010) identified E196C, L198C, and I202C (all external to R1) that were accessible externally preferentially in the open state, suggesting that S4 moves outward and/or rotates. However, a smaller probe for accessibility, *n*-ethylmaleimide (NEM) in a PEGylation protection assay, revealed that all S4 residues external to position 203 (including the three mentioned above) are accessible, presumably in the closed state (Kurokawa and Okamura, 2014). It should be noted that the former study examined kinetics of MTS effects under voltage clamp, so the gating state was well defined. In the latter study, voltage clamp was not involved, and although at 0 mV most WT channels are closed, many mutations shift the g_H–V relationship, and thus mutant channels could be open at 0 mV.

Accessibility assays are limited by the size of the probe but will also be influenced by charge. For example, aqueous accessibility determined by Cys scanning with NEM as a probe revealed greater accessibility than when using the larger AMS (4-acetamido-4′-maleimidylstilbene-2,2′-disulfonic acid) as a probe (Kurokawa and Okamura, 2014). Furthermore, Ag^+ as a probe revealed much greater accessibility than the larger NEM (Fillingame et al., 2002). Fillingame et al. (2002) point out that because Ag^+ has an ionic radius like H_3O^+, it is ideal for probing proton pathways. Zn^{2+} has a smaller ionic radius than Ag^+ (Robinson and Stokes, 1959) but is divalent. As a probe of H_V1, it reveals greater accessibility than the bulkier MTS reagents (Kulleperuma et al., 2013; Morgan et al., 2013). In bulk solution, the proton

Downloaded from http://rupress.org/jgp/article-pdf/148/2/97/1795854/jgp_201611619.pdf by guest on 08 February 2026

Table 5. **Changes in H_V1 properties in S3 (166–188) and S3–S4 linker (189–196) mutants versus WT channels**

Mutant	Species	Expr. system	$I_H^?$	τ_{act}	τ_{tail}	ΔV_{thr}	ΔpH slope	Selectivity	Other	Reference
E164A/E171A	hH_V1	HEK wc	Yes			−7				Ramsey et al., 2010
H167N/H168V/K169N	hH_V1	HEK wc	Yes			−13	44			Ramsey et al., 2010
E171A/D174A	hH_V1	HEK wc	Yes			−116	39			Ramsey et al., 2010
E171A	hH_V1	Vesicle flux							Δ H^+ flux[a]	Letts, 2014
D174A	hH_V1	HEK wc	Yes			−111	38			Ramsey et al., 2010
D174A	hH_V1	Vesicle flux							Δ H^+ flux[a]	Letts, 2014
D174N	hH_V1	HEK wc	Yes			−142	36			Ramsey et al., 2010
D174H	hH_V1	HEK wc	Yes			−136	37			Ramsey et al., 2010
D174E	hH_V1	HEK wc	Yes			−52	46			Ramsey et al., 2010
D174A	CiH_V1 [D222A]	*Xenopus* TEVC	Yes			−111				Chamberlin et al., 2014
D174C/R205C	CiH_V1 [D222C/R255C]	*Xenopus* TEVC	Yes			−95				Chamberlin et al., 2014
D174C/R208C	CiH_V1 [D222C/R258C]	*Xenopus* TEVC	Yes			48				Chamberlin et al., 2014
V178A	hH_V1	*Xenopus* i-o	Yes			−27				Hong et al., 2014
D112V/V178D	hH_V1	COS/HEK wc	No							Morgan et al., 2013
S181A	hH_V1	HEK wc	Yes			18	46			Ramsey et al., 2010
S181A	hH_V1	*Xenopus* i-o	Yes			0				Hong et al., 2014
D112V/S181D	hH_V1	COS/HEK wc	No							Morgan et al., 2013
F182A	hH_V1	*Xenopus* i-o	Yes			−9				Hong et al., 2014
D185A	hH_V1	HEK wc	Yes			58	47			Ramsey et al., 2010
D185M	hH_V1	COS/HEK wc	Yes					H^+		Musset et al., 2011
D185V	hH_V1	COS/HEK wc	Yes			20[b]	43[b]	H^+		Musset et al., 2011
D185A	hH_V1	COS/HEK wc	Yes			42[b]	40[b]	H^+		Musset et al., 2011
D185A	hH_V1	Vesicle flux							nc H^+ flux	Letts, 2014
D185N	hH_V1	COS/HEK wc	Yes			36[b]	47[b]	H^+		Musset et al., 2011
D185C	CiH_V1 [D233C]	*Xenopus* TEVC	Yes			76				Chamberlin et al., 2014
E185C/R208C	CiH_V1 [D233C/R258C]	*Xenopus* TEVC	Yes			4				Chamberlin et al., 2014
E192A/E196A	hH_V1	HEK wc	Yes			13				Ramsey et al., 2010
H193A	hH_V1	HEK wc	Yes					H^+	39 × K_d Zn^{2+}	Ramsey et al., 2006
H193A	hH_V1	Vesicle flux							nc H^+ flux	Letts, 2014
H140A/H193A	hH_V1	HEK wc	Yes			−12	46	H^+	2,000 × K_d Zn^{2+}	Ramsey et al., 2006

That numerical entries are shown does not imply that any given change was significant. Italicized mutant entries from nonhuman species show the hH_V1 equivalent. In the Expression system column: HEK, HEK-293, HEK-293T, tsA, or HM1; COS, COS-7; *Xenopus*, *Xenopus laevis* oocyte; wc, whole cell; i-o, inside-out patch configuration; TEVC, two-electrode voltage clamp. Blank entries indicate that the parameter was not examined. nc, measured, but no change. Parameters are given relative to WT in each study. For $I_H^?$, yes means currents are detectable. Time constants are ratios of mutant/WT. The $\Delta V_{threshold}$ value is the change in absolute position of the g_H–V relationship versus WT. The ΔpH slope is the slope in millivolts of the relationship between $V_{threshold}$ (or other parameters reflecting the absolute position of the g_H–V relationship) versus V_{rev} or E_H (which are not identical; see section Table entries defined).

[a]Normal initial H^+ flux followed by recovery ascribed to leak induced in vesicles.

[b]Previously unpublished, analyzed from data for Musset et al. (2011).

diffuses almost exclusively as protonated buffer (DeCoursey, 1991; DeCoursey and Cherny, 1994, 1996). One expects that the proton permeates the aqueous vestibules of H_V1 as H_3O^+ (DeCoursey, 2003b) and the selectivity filter as H^+ (Dudev et al., 2015).

Internal accessibility assessed rigorously by Cys scanning and MTS reaction kinetics under voltage clamp indicated that *I212C* and *N214C* were both more accessible at negative voltages, indicating greater accessibility in closed channels (Gonzalez et al., 2010). The residues with state-dependent accessibility in S4 thus span two positions internally and four externally. These results strongly support the idea that S4 moves outwardly during opening, but the extent of movement could be one turn of the helix, consistent with the "one-click" model (Li et al., 2015). Also consistent with a small excursion of S4 during opening are studies using Zn^{2+} to probe for accessibility of Arg→His mutants. In hH_V1, R205H was externally accessible and R208H was accessible externally and possibly also internally (currents were tiny), whereas R211H was accessible only internally even in the open state (Kulleperuma et al., 2013; Morgan et al., 2013).

Accessibility of S1 was explored by Cys scanning, and five residues were found to be more accessible at positive (open) voltages (Mony et al., 2015). One was external, and the rest were internal. Although the internal residues span seven positions, the fact that both the external and internal residues were more exposed in open channels suggests a widening of the vestibules rather than a large inward translational movement.

Gating charge. Numerous mutations have been performed in the S4 helix with the goal of determining the extent to which channel opening involves outward movement of positively charged groups in S4 during depolarization, as is thought to occur in most other voltage-gated ion channels. Each of the three Arg in S4 has

Downloaded from http://rupress.org/jgp/article-pdf/148/2/97/1795854/jgp_201611619.pdf by guest on 08 February 2026

Table 6. **Changes in H_V1 properties in S4 (197–218) mutants versus WT channels**

Mutant	Species	Expr. system	*I*?	τ_{act}	τ_{tail}	ΔV_{thr}	ΔpH slope	Selectivity	Other	Reference
E196C	CiH_V1 [A246C]	*Xenopus* TEVC	Yes						MTS_o open>closed	Gonzalez et al., 2010
L198C	CiH_V1 [I248C]	*Xenopus* TEVC	Yes						MTS_o open>closed	Gonzalez et al., 2010
G199C	CiH_V1 [G249C]	*Xenopus* i-o	Yes			2				Mony et al., 2015
L200W	CiH_V1 [L250W]	*Xenopus* TEVC	Yes	0.27	0.67					Okuda et al., 2016
L200W/ΔC	CiH_V1 [L250W/ΔC]	*Xenopus* TEVC	Yes	0.20	0.019					Okuda et al., 2016
I202C	CiH_V1 [V252C]	*Xenopus* TEVC	Yes						MTS_o open>closed	Gonzalez et al., 2010
R205A	hH_V1	HEK wc	Yes	0.0053	0.086	−1	48		0.63 × WT gating charge[a]	Ramsey et al., 2006, 2010
R205A	hH_V1	Vesicle flux							Δ H^+ flux[b]	Letts, 2014
R205H[c]/T222stop	hH_V1	COS wc	Yes					H^+	Accessible to external Zn^{2+}	Kulleperuma et al., 2013
R205Q	Mouse [R201Q]	HEK wc	Yes	Faster		−50			1.36 × WT gating charge[a]	Sasaki et al., 2006
R205N	CiH_V1 [R255N]	*Xenopus* i-o	Yes						0.33 × WT gating charge[d]	Gonzalez et al., 2013
R205N	CiH_V1 [R255N]	*Xenopus* TEVC	Yes			−36			0.78 × WT gating charge[a]	Chamberlin et al., 2014
R205C	CiH_V1 [R255C]	*Xenopus* TEVC	Yes			−37			1.3 × WT gating charge[a]	Chamberlin et al., 2014
R205A/R208A	hH_V1	HEK wc	Yes			128	51			Ramsey et al., 2010
R205A/R211A	hH_V1	HEK wc	Yes			96	45			Ramsey et al., 2010
L206C	CiH_V1 [L256C]	*Xenopus* TEVC	Yes						No $MTS_{o/i}$ access	Gonzalez et al., 2010
W207A,[c] W207S,[c] or W207F[c]	hH_V1	HEK/COS wc	Yes	0.01	0.034	−17.9	40	H^+	Loss of selectivity at $pH_o > 8$	Cherny et al., 2015
W207I	Mouse [W203I]	HEK wc	Yes	0.019	0.059				Tandem dimer	Okuda et al., 2016
W207A, W207S, or *W207F*	kH_V1 [W176A, W176S, W176F]	HEK/COS wc	Yes	0.025			40	H^+		Cherny et al., 2015
W207A, W207S, or *W207F*	EhH_V1 [W278A, W278S, W278F]	HEK/COS wc	Yes	0.2		−28.2	50	H^+		Cherny et al., 2015
W207I	CiH_V1 [W257I]	*Xenopus* TEVC	Yes	0.29	0.030					Okuda et al., 2016
W207I/A210A	CiH_V1 [W257I/F260A]	*Xenopus* TEVC	Yes	0.23	0.026					Okuda et al., 2016
R208A	hH_V1	HEK wc	Yes	0.0965	0.075	7	45			Ramsey et al., 2006, 2010
R208A	hH_V1	Vesicle flux							Δ H^+ flux[b]	Letts, 2014
R208A	hH_V1	*Xenopus* i-o	No							Hong et al., 2014
R208K	hH_V1	*Xenopus* i-o	Yes			−40			1.7 × WT gating charge[a]	Hong et al., 2014
R208K	hH_V1	HEK/COS wc	Yes					H^+		Dudev et al., 2015
R208H[c]/T222stop	hH_V1	COS wc	Yes					H^+	Accessible to external & maybe internal Zn^{2+}	Kulleperuma et al., 2013
R208Q	hH_V1	*Xenopus* i-o	No							Hong et al., 2014
R208Q	Mouse [R204Q]	HEK wc	No							Sasaki et al., 2006
R208N	hH_V1	*Xenopus* i-o	No							Hong et al., 2014
R208N	CiH_V1 [R258N]	*Xenopus* i-o	Yes						0.50 × WT gating charge[d]	Gonzalez et al., 2013
R208C	CiH_V1 [R258C]	*Xenopus* TEVC	Yes			−10			0.87 × WT gating charge[a]	Chamberlin et al., 2014
V209C	CiH_V1 [V259C]	*Xenopus* TEVC	Yes						No $MTS_{o/i}$ access	Gonzalez et al., 2010
R211A	hH_V1	HEK wc	Yes	2.24	0.092	70	53			Ramsey et al., 2006, 2010
R211A	hH_V1	Vesicle flux							Δ H^+ flux[b]	Letts, 2014
R211S	hH_V1	*Xenopus* i-o	Yes			35			0.72 × WT gating charge[a]	Hong et al., 2014
R211S	hH_V1	*Xenopus* i-o	Yes			87	49	Gu^+	at pH 8//8	Berger and Isacoff, 2011
R211S/I127C	CiH_V1 [R261S/I175C]	*Xenopus* i-o	Yes			15				Mony et al., 2015
R211H[c]/T222stop	hH_V1	COS wc	Yes					H^+	Accessible to internal Zn^{2+} when open	Kulleperuma et al., 2013
R211H/D112V/V116D[c]	hH_V1	COS/HEK wc	Yes						Accessible to internal Zn^{2+} when open	Morgan et al., 2013
R211Q	mH_V1 [R207Q]	HEK wc	Yes			nc				Sasaki et al., 2006
R211N	CiH_V1 [R261N]	*Xenopus* i-o	Yes						0.38 × WT gating charge[d]	Gonzalez et al., 2013
R211C	CiH_V1 [R261C]	*Xenopus* TEVC	Yes			54		H^+	0.78 × WT gating charge[a]	Chamberlin et al., 2014
R211C	NpHv1 [R163C]	HEK wc	Yes					H^+		Chaves et al., 2016

Downloaded from http://rupress.org/jgp/article-pdf/148/2/97/1795854/jgp_201611619.pdf by guest on 08 February 2026

Table 6. **Changes in H_V1 properties in S4 (197–218) mutants versus WT channels** *(Continued)*

Mutant	Species	Expr. system	$I_?$	τ_{act}	τ_{tail}	ΔV_{thr}	ΔpH slope	Selectivity	Other	Reference
I212C	CiH_V1 [I262C]	*Xenopus* TEVC	Yes						MTS_i closed>open	Gonzalez et al., 2010
N214K	hH_V1	HEK wc	Yes			−3	43		Inward rectification	Ramsey et al., 2010
N214R	hH_V1	HEK wc	Yes			10	40		Inward rectification	Ramsey et al., 2010
N214R	hH_V1	*Xenopus* i-o	No							Tombola et al., 2008
N214A	hH_V1	HEK wc	Yes			−3	42			Ramsey et al., 2010
N214A	hH_V1	Vesicle flux							nc H^+ flux	Letts, 2014
N214R	mH_V1 [N210R]	HEK wc	Yes	Slow	Very slow	−V		H^+		Sakata et al., 2010
N214D	hH_V1	COS/HEK wc	Yes					H^+		Musset et al., 2011
N214C	CiH_V1 [N264C]	*Xenopus* TEVC	Yes						MTS_i closed>open	Gonzalez et al., 2010
G215A	hH_V1	COS/HEK wc	Yes		Fast			H^+		Musset et al., 2011
I217stop	mH_V1 [I213stop]	HEK wc	Yes							Sakata et al., 2010
G215stop	mH_V1 [G211stop]	HEK wc	Yes							Sakata et al., 2010
I213stop	mH_V1 [I209stop]	HEK wc	Yes							Sakata et al., 2010
A210stop	mH_V1 [A206stop]	HEK wc	Yes			+V		H^+	τ_{act} has weak V dependence	Sakata et al., 2010
L204stop	mH_V1 [L200stop]	HEK wc	No							Sakata et al., 2010

That numerical entries are shown does not imply that any given change was significant. Italicized mutant entries from nonhuman species show the hH_V1 equivalent. HEK, HEK-293, HEK-293T, tsA, or HM1; COS, COS-7; *Xenopus*, *Xenopus laevis* oocyte; wc, whole cell; i-o, inside-out patch configuration; TEVC, two-electrode voltage clamp. Blank entries indicate that the parameter was not examined. nc, measured, but no change. Parameters are given relative to WT in each study. For $I_?$, yes means currents are detectable. Time constants are ratios of mutant/WT. The $\Delta V_{threshold}$ value is the change in absolute position of the g_H–V relationship versus WT. The ΔpH slope is the slope in millivolts of the relationship between $V_{threshold}$ (or other parameters reflecting the absolute position of the g_H–V relationship) and V_{rev} or E_H (which are not identical; see section Table entries defined). When C-terminal truncations are indicated as XNNNstop, this means STOP replaces X at position NNN; hence, position NNN and all subsequent residues are truncated, and the last position remaining is NNN-1. For column Other, MTS access from inside or outside (MTS_i or MTS_o, respectively) is listed as open>closed if the open channel was more accessible.

[a]Slope factor of g_H–V relationship.

[b]Normal initial H^+ flux followed by recovery ascribed to leak induced in vesicles.

[c]In an H140A/H193A (Zn^{2+} insensitive) background.

[d]By limiting slope method.

been mutated, and the effect on gating charge was evaluated in various ways. Unfortunately, the methods for estimating gating charge are challenging, and several problems unique to H_V1 make the task even more difficult. A direct approach is to measure the integral of the gating current and divide by the number of channels. However, it is nearly impossible to measure gating current in H_V1 because the permeant ion cannot be removed, simple blockers have not been identified, and gating is extremely slow. The most potent inhibitor, Zn^{2+}, does not occlude the pore, as would be required to reveal gating charge, but rather shifts the g_H–V relationship positively and slows activation (Cherny and DeCoursey, 1999). Block by guanidine derivatives is also state dependent (Hong et al., 2013). Another procedure that is technically straightforward but of limited information value is to determine the slope factor of a Boltzmann function fit to the g_H–V relationship. The slope factor does include the effective gating charge, but in a highly model-dependent manner; nevertheless, the steepness of the voltage dependence should diminish if gating charges are removed by mutation. Such estimates are indicated in Table 6 by footnote b. There are numerous pitfalls in this measurement, a major one being proton depletion, which produces artificial saturation of current (DeCoursey, 1991; DeCoursey and Cherny, 1994; Musset et al., 2008a), and at best, the slope provides a model-dependent estimate that almost always underestimates the true gating charge (Bezanilla and Villalba-Galea, 2013). Early studies reported slope factors corresponding to a gating charge of 1.4 e_0 (Sasaki et al., 2006) for WT mH_V1 or 0.9 e_0 for WT hH_V1 (Ramsey et al., 2006). A more meaningful approach for H_V1 has been the limiting slope method, devised by Wolf Almers (Almers, 1978). This method works for a wide range of gating models, but not all (Sigg and Bezanilla, 1997), and provides gating charge estimates of ∼6 e_0 for native rat proton currents (DeCoursey and Cherny, 1996, 1997), for CiH_V1 (Gonzalez et al., 2010), and for hH_V1 (Musset et al., 2008a) and 4 e_0 for mH_V1 (Fujiwara et al., 2012). The difficulty is mainly that measurements need to be extended to large negative voltages to achieve sufficiently low g_H values to determine the limiting slope. When critical amino acids such as the Arg in S4 are mutated, the resulting currents are often quite small, which leads to underestimates of the gating charge. Another vexing source of error is that mutation, for example, of Arg^{205} (R255N in CiH_V1) appears to reduce the extent of S4 movement during gating (Gonzalez et al., 2013), which in retrospect is not a very surprising result of removing one of the charges in the protein thought to move in response to voltage changes!

Three studies reported lower gating charge (Ramsey et al., 2006; Gonzalez et al., 2013; Chamberlain et al., 2014) and two reported higher gating charge (Sasaki et

Downloaded from http://rupress.org/jgp/article-pdf/148/2/97/1795854/jgp_201611619.pdf by guest on 08 February 2026

al, 2006; Chamberlain et al, 2014) when Arg^{205} was neutralized (Table 6). Two studies reported lower gating charge when Arg^{208} was neutralized (Gonzalez et al., 2013; Chamberlain et al., 2014). The conservative Arg→Lys mutation increased gating charge by 70% (Hong et al., 2014). Finally, both studies of neutralized Arg^{211} reported lower gating charge (Gonzalez et al., 2013; Chamberlain et al., 2014). It might be noted that all studies reporting higher gating charge were based on the slope of Boltzmann functions. The tables do not list a number of studies of monomeric constructs, which consistently exhibit only half the gating charge of native dimers, a manifestation of cooperative gating (Gonzalez et al., 2010, 2013; Fujiwara et al., 2012; Okuda et al., 2016).

Why is there a Trp in the middle of S4? Tryptophan prefers the interfacial environment near membrane lipid head groups (Landolt-Marticorena et al., 1993; Killian and von Heijne, 2000), but in H_V1, a perfectly conserved Trp residue (Trp^{207} in hH_V1) is located right in the middle of the S4 TM helix. Two studies have been conducted to determine why it is there, exploring mutations in multiple species (Table 1). The most prominent effect of Trp mutation was drastic acceleration of channel gating. In hH_V1, activation and deactivation were 100 times and 30 times faster, respectively (Cherny et al., 2015), whereas in CiH_V1, deactivation was more profoundly accelerated (Okuda et al., 2016). Effects of Trp mutation differ dramatically among species. Table 6 shows that the acceleration of channel opening was 100-fold in hH_V1, 5-fold in EhH_V1, 40-fold in kH_V1 (Cherny et al., 2015), 3.4-fold in CiH_V1, and 53-fold in mH_V1 (Okuda et al., 2016). It is noteworthy that the properties of W207A, W207S, and W207F (three substituents with quite different properties) were all modified identically in hH_V1 and in kH_V1, which strongly implicates a unique property of Trp at this location (Cherny et al., 2015). Two mechanisms have been proposed to explain how Trp slows gating. Based on the proximity of Trp^{207} and Arg^{211} in the closed crystal structure (Takeshita et al., 2014), cation–π interaction between Trp^{207} and Arg^{211} was postulated to stabilize closed hH_V1 channels, with this interaction broken during channel opening (Cherny et al., 2015). In CiH_V1, π stacking of Trp from each protomer at the dimer interface was proposed to slow deactivation (Okuda et al., 2016). This proposal was supported by Trp slowing deactivation preferentially in dimeric versus monomeric constructs (Okuda et al., 2016). Mutant cycle analysis supported the idea that π stacking of Trp at the dimer interface contributed to slow deactivation, but the slowing of activation was independent of channel dimerization. Consistent with this latter conclusion, kH_V1 lacks predicted coiled coil in its C terminus and thus is likely a monomer (Smith and DeCoursey, 2013), and τ_{act} was two orders of magnitude faster in Trp mutants of kH_V1.

Trp^{207} mutants not only opened and closed faster, but the Q_{10} of their gating kinetics dropped from the astronomical 6–9 of WT H_V1 (DeCoursey and Cherny, 1998; Ramsey et al., 2006; Kuno et al., 2009) into the realm of ordinary voltage-gated ion channels, 3.5–4.0 (Cherny et al., 2015). Trp^{207} is a key component in several of the unique properties of H_V1 (Cherny et al., 2015).

Does Arg^{211} contribute to proton selectivity? One study concluded that Arg^{211} is part of the selectivity filter because 15 R211x mutants were permeable to guanidinium, Gu^+, at symmetrical pH 8, whereas outward current in WT hH_V1 expressed in *Xenopus* oocytes was blocked (Berger and Isacoff, 2011). However, this result could not be reproduced in hH_V1 expressed in HEK cells, suggesting that the expression system alters this property. Large outward currents were seen in both WT and R211A channels in HEK cells at high pH (DeCoursey, 2013). Neither WT nor R211A was detectably permeant to smaller cations (unpublished data), so the Gu^+ result appears anomalous, perhaps related to the ability of this chaotropic ion to disrupt hydrogen bonds, interact with hydrophobic regions of proteins, bind to sites normally occupied by water, and denature proteins (Makhatadze and Privalov, 1992; Courtenay et al., 2001; England and Haran, 2011). Although molar Gu^+ is typically required for wholesale denaturation, 50 mM Gu^+ sufficed to perturb the permeation pathway of voltage-gated K^+ channels (Kalia and Swartz, 2011). It is likely that ions are highly concentrated in the pores of channels just as they are in the active sites of enzymes (Jimenez-Morales et al., 2012) because of the high charge density in the protein. We imagine that Gu^+ tunnels through the pore in a manner that no physiological ion can reproduce, perhaps by breaking the hydrogen bonds between Asp^{112} and Arg^{208} that prevent ions other than H_3O^+ from entering the selectivity filter (Dudev et al., 2015).

It is difficult to imagine a role for Arg^{211} in selectivity because the C terminus can be truncated along with the inner part of S4 (between Arg^{208} and Arg^{211}) without loss of selectivity (Sakata et al., 2010). One might argue that when Arg^{211} is removed, Arg^{208} may take over its function. However, R211H in hH_V1 (Kulleperuma et al., 2013) and R211C in NpH_V1 (Chaves et al., 2016) and CiH_V1 (Chamberlin et al., 2015) are all proton selective.

What about Asn^{214}? In S4, where many VSD-containing proteins have a fourth Arg or Lys (Table 1), H_V1 has Asn^{214}. Noting that the N214R mutant did not conduct, an early suggestion was that, assuming that S4 in H_V1 moves outward as it does in other channels, Asn^{214} might occupy a narrow constriction where it would allow protons to pass (Tombola et al., 2008). Two other groups reported that N214R did conduct (Ramsey et al., 2010; Sakata et al., 2010), but both used mammalian expression systems, as opposed to *Xenopus*. This may

Downloaded from http://rupress.org/jgp/article-pdf/148/2/97/1795854/jgp_201611619.pdf by guest on 08 February 2026

be another example in which the expression system alters the outcome. However, the currents in N214R mutants were small, so this may be a case of different laboratories having different definitions of what comprises a detectable current. Given evidence that Arg^{211} remains internally accessible in open hH_V1 (Kulleperuma et al., 2013; Morgan et al., 2013; Li et al., 2015), Asn^{214} most likely remains well inside the internal vestibule.

Table 7: The C terminus (positions 219–273)

The coiled-coil region holds the dimer together. The C terminus of hH_V1 contains extensive typical coiled-coil sequences. When it was learned that mammalian and some other H_V1 assemble into dimers in cell membranes, the coiled-coil regions were implicated in dimerization (Koch et al., 2008; Lee et al., 2008; Tombola et al., 2008; Li et al., 2010). A cross-linking study with 15 strategically located Cys mutants confirmed that the C terminus was a major point of attachment of the dimer (Lee et al., 2008). By modifying the C terminus, Okamura's group was able to generate functioning trimers and tetramers (Fujiwara et al., 2013a). A crystal structure of the C terminus revealed that the lone Cys (Cys^{249} in hH_V1) in the C terminus forms a disulfide bond, increasing the stability of the dimer (Fujiwara et al., 2013b). This result was confirmed by mutation of the two native Cys in hH_V1; C107S was still 90% dimer, whereas C249S was <5% dimer (Li et al., 2015).

C terminus truncation was determined to produce mainly monomeric constructs (Koch et al., 2008; Tombola et al., 2008). The monomers behave differently electrophysiologically because the dimer exhibits cooperative gating (Gonzalez et al., 2010; Tombola et al., 2010). The dimer opens with sigmoid kinetics, like a classical Hodgkin-Huxley n^2 mechanism (Hodgkin and Huxley, 1952). The monomer opens approximately five times faster and with exponential kinetics (Koch et al., 2008; Musset et al., 2010b,c; Tombola et al., 2010; Fujiwara et al., 2012). Because both monomers must move in response to voltage before either can open, the gating charge is twice as large in the dimer as in the monomer (Gonzalez et al., 2010, 2013; Fujiwara et al., 2012; Okuda et al., 2016).

Does the C terminus modulate gating? The Okamura group has studied the C terminus extensively using creative approaches. They conclude that the C terminus and the S4 helix form a single rigid monolithic rod, which moves during cooperative gating (Fujiwara et al., 2012, 2014). Two types of evidence support this conclusion. First, when a rigid (AAA) or flexible (GGG) triplet was inserted between S4 and the C terminus (at 220–222, replacing VKT; Table 7), the rigid linker behaved like a WT dimer (sigmoid kinetics, slow activation, and full gating charge), whereas the floppy linker produced monomer-like behavior (exponential kinetics, fast activation, and half the gating charge). This showed that simply being a dimer was insufficient to produce cooperative gating; a continuous α helix from the C terminus through S4 was required (Fujiwara et al., 2012). In another intriguing study, 1–10 amino acids were inserted or deleted from the connection between the S4 TM segment and the C terminus. Gating kinetics exhibited a periodic dependence on the linker length, presenting slower WT-like kinetics when the whole S4-C domain was in register (Fujiwara et al., 2014). In this context, even though the VSD-only construct (lacking both N and C termini) spontaneously associates into dimers in liposomes (Li et al., 2015), it likely still functions as two independent monomers.

There is also evidence that interactions at the extracellular end of the S1 segment contribute to the dimer interface (Lee et al., 2008; Qiu et al., 2013; Hong et al., 2015). To enable this to occur, the outer ends of S4 were proposed to relax or unwind (Hong et al., 2015).

General conclusions and remaining questions

A large number of mutations result in functional proton channels. This might be inferred from the fact that there are sequence differences at most positions in H_V1 among different species (Smith et al., 2011). Perhaps not surprisingly, mutations that produce nonfunctional protein tend to occur at highly conserved positions and often involve changes in charge. Both Arg^{208} mutation (Table 6) and Asp^{112} mutation (Table 3) are severely detrimental to H_V1 function, which we ascribe to both their central location and essential roles in proton permeation (Kulleperuma et al., 2013; Morgan et al., 2013; Dudev et al., 2015).

Several examples exist in which H_V1 channels apparently behave differently in mammalian and amphibian expression systems. Whether these discrepancies reflect differences in as yet unknown posttranslational modification can only be speculated.

Charge, countercharge, and contra-countercharge. Electrostatics is clearly of central importance in ion channel function. Voltage sensing almost certainly involves charged groups within the membrane electrical field. The idea that interaction of charge pairs (oppositely charged) helps stabilize open or closed states is well entrenched among enthusiasts of H_V1 as well as other voltage-gated ion channels (Papazian et al., 1995; Tiwari-Woodruff et al., 1997). It seems reasonable to conclude that mutations that neutralize a charge will preclude this element from performing this function. The extensive study by Ramsey et al. (2010) together with other table entries is consistent with the interpretation that Asp^{112}, Glu^{119}, Asp^{123}, and Asp^{185} in the outer vestibule stabilize the open state; internally accessible

Downloaded from http://rupress.org/jgp/article-pdf/148/2/97/1795854/jgp_201611619.pdf by guest on 08 February 2026

Table 7. **Changes in H_V1 properties in C-terminal (219–273) mutants versus WT channels**

Mutant	Species	Expr. system	I_H	τ_{act}	τ_{tail}	ΔV_{thr}	ΔpH slope	Selectivity	Other	Reference
S219P	hH_V1	COS/HEK wc	Yes					H^+		Musset et al., 2011
C249S	hH_V1								Loss of dimer formation	Li et al., 2015
ΔC (T222stop)	hH_V1	HEK wc	Yes			1	28			Ramsey et al., 2010
ΔC (T222stop)	hH_V1		Yes	0.15					Weaker Zn^{2+} effects	Musset et al., 2010b
ΔC	mH_V1 (V216stop)	HEK wc	Yes	0.34		nc	nc		Loss of dimer formation	Koch et al., 2008
ΔC	mH_V1 (V216stop)	HEK wc	Yes	0.15	0.16					Okuda et al., 2016
ΔC	CiH_V1 (D275stop)	*Xenopus* TEVC	Yes	0.14	0.075					Okuda et al., 2016
V220G/K221G/T222G	mH_V1 V216G/K217G/T218G	HEK wc							Loss of cooperative gating	Fujiwara et al., 2012

That numerical entries are shown does not imply that any given change was significant. HEK, HEK-293, HEK-293T, tsA, or HM1; COS, COS-7; *Xenopus, Xenopus laevis* oocyte; wc, whole cell; i-o, inside-out patch configuration; o-o, outside-out patch configuration; TEVC, two-electrode voltage clamp. Blank entries indicate that the parameter was not examined. nc, measured, but no change. Parameters are given relative to WT in each study. For I_H, yes means currents are detectable. Time constants are ratios of mutant/WT. The $\Delta V_{threshold}$ value is the change in absolute position of the g_H–V relationship versus WT. The ΔpH slope is the slope in millivolts of the relationship between $V_{threshold}$ (or other parameters reflecting the absolute position of the g_H–V relationship) and V_{rev} or E_H (which are not identical; see section Table entries defined). When C-terminal truncations are indicated as XNNNstop, this means STOP replaces X at position NNN; hence, position NNN and all subsequent residues are truncated, and the last position remaining is NNN-1. The mouse N-terminal deletions were done by replacing P78M to initiate translation at that position. Note that a large number of mutations to the linker between S4 and the C terminus have been studied (Fujiwara et al., 2012, 2014), but their results are beyond the scope of this table and thus are not included.

acidic groups (Glu^{153} and Asp^{174}) more strongly stabilize the closed state. Interacting external and internal charge clusters have been observed consistently in MD simulations of H_V1 (Ramsey et al., 2010; Kulleperuma et al., 2013; Morgan et al., 2013; Chamberlin et al., 2014).

However, large shifts of the g_H–V relationship can also be observed upon replacing one uncharged residue with another one (e.g., F150W in Table 4). In fact, almost every mutation that has been examined changes $V_{threshold}$ one way or the other. Pless et al. (2011) showed convincingly that two highly conserved acids in the Shaker K^+ channel VSD (equivalent to Glu^{153} and Asp^{174} in hH_V1; Table 1) could be neutralized with little effect on the g_K–V relationship. Four external and two internal acidic residues were identified here as counterchanges based on the observation that in neutral mutants the g_H–V relationship shifted in the predicted direction; thus, by this definition, the mechanism appears to involve charge. Alternatively, these charged groups might function primarily to create an aqueous vestibule and consequently a highly focused electrical field (Pless et al., 2011). We cannot resolve the mechanism without strategically designed experiments. If the function of the acidic residues is to create aqueous vestibules, one might predict that polar substituents that replace charges should produce less drastic effects than nonpolar ones. Mining the tables, we find that existing data are neither extensive nor self-consistent enough to provide a clear answer. The reported g_H–V relationship shifts (polar vs. nonpolar) are as follows: Asp^{112} (31, 23, 13, and 25 vs. 59, 41, and 44); Asp^{185} (36 vs. 58, 20, 42, and 76); Glu^{153} (−117 vs. −55, −55, and −101), and Asp^{174} (−142 and −136 vs. −111 and −111). Another point is that Lys^{157} is predicted by MD to be involved in an internal salt bridge in closed H_V1 (Chamberlin et al., 2014), yet its neutralization has little effect on the g_H–V relationship (Table 4). This question clearly requires future study.

Outstanding remaining problems. It seems surprising that the N terminus contains several sites that influence gating, despite being topologically remote from S4 (at least in the image in Fig. 1). It also seems paradoxical that truncation of the entire N terminus has less overt effect than point mutations within the N terminus. However, the N terminus is disordered, and its tertiary structure is unknown. How it interacts with the rest of the molecule is completely unknown. For example, how does phosphorylation of Thr^{29} alter gating so profoundly? Why does the innocuous-appearing M91T mutation impede hH_V1 activation?

Voltage gating is a difficult structure–function problem because it is dynamic, not to mention three-dimensional. Despite Cys scanning and other studies designed to examine state-dependent accessibility and molecular movement, it remains unclear which parts of the H_V1 molecule move during channel opening (S4, S1?), in which direction, and how far. For example, accessibility may change as a result of movement "up" or "down," or into or out of a hydrophobic region, but it can also change simply by expansion or contraction of an aqueous vestibule, or by the helix rotating toward or away from an aqueous space.

Although much has been learned about selectivity and a model has been proposed (Dudev et al., 2015), questions still remain. Is the model correct? Do other parts of the channel contribute to selectivity? Where is the rate-limiting point of the permeation pathway?

Without a doubt, the most important question remains completely unsolved; namely, the mechanism of ΔpH-dependent gating. This unique ΔpH dependence is crucial to all of the known biological functions of H_V1.

Downloaded from http://rupress.org/jgp/article-pdf/148/2/97/1795854/jgp_201611619.pdf by guest on 08 February 2026

ACKNOWLEDGMENTS

We appreciate helpful corrections and comments provided by I. Scott Ramsey and Robert H. Fillingame.

This work was supported by National Institutes of Health grant GM102336 and National Science Foundation grant MCB-1242985.

The authors declare no competing financial interests.

Author contributions: T.E. DeCoursey wrote the paper. D. Morgan, B. Musset, and V.V. Cherny analyzed existing data for Tables 3 and 5. All authors read and approved the manuscript.

Lesley C. Anson served as editor.

Submitted: 4 May 2016
Accepted: 30 June 2016

REFERENCES

Alabi, A.A., M.I. Bahamonde, H.J. Jung, J.I. Kim, and K.J. Swartz. 2007. Portability of paddle motif function and pharmacology in voltage sensors. *Nature.* 450:370–375. http://dx.doi.org/10.1038/nature06266

Almers, W. 1978. Gating currents and charge movements in excitable membranes. *Rev. Physiol. Biochem. Pharmacol.* 82:96–190.

Balashov, S.P., L.E. Petrovskaya, E.S. Imasheva, E.P. Lukashev, A.K. Dioumaev, J.M. Wang, S.V. Sychev, D.A. Dolgikh, A.B. Rubin, M.P. Kirpichnikov, and J.K. Lanyi. 2013. Breaking the carboxyl rule: lysine 96 facilitates reprotonation of the Schiff base in the photocycle of a retinal protein from *Exiguobacterium sibiricum*. *J. Biol. Chem.* 288:21254–21265. http://dx.doi.org/10.1074/jbc.M113.465138

Bánfi, B., J. Schrenzel, O. Nüsse, D.P. Lew, E. Ligeti, K.H. Krause, and N. Demaurex. 1999. A novel H^+ conductance in eosinophils: Unique characteristics and absence in chronic granulomatous disease. *J. Exp. Med.* 190:183–194. http://dx.doi.org/10.1084/jem.190.2.183

Berger, T.K., and E.Y. Isacoff. 2011. The pore of the voltage-gated proton channel. *Neuron.* 72:991–1000. http://dx.doi.org/10.1016/j.neuron.2011.11.014

Bezanilla, F., and C.A. Villalba-Galea. 2013. The gating charge should not be estimated by fitting a two-state model to a *Q-V* curve. *J. Gen. Physiol.* 142:575–578. http://dx.doi.org/10.1085/jgp.201311056

Byerly, L., R. Meech, and W. Moody Jr. 1984. Rapidly activating hydrogen ion currents in perfused neurones of the snail, *Lymnaea stagnalis*. *J. Physiol.* 351:199–216. http://dx.doi.org/10.1113/jphysiol.1984.sp015241

Capasso, M., M.K. Bhamrah, T. Henley, R.S. Boyd, C. Langlais, K. Cain, D. Dinsdale, K. Pulford, M. Khan, B. Musset, et al. 2010. HVCN1 modulates BCR signal strength via regulation of BCR-dependent generation of reactive oxygen species. *Nat. Immunol.* 11:265–272. http://dx.doi.org/10.1038/ni.1843

Capasso, M., T.E. DeCoursey, and M.J.S. Dyer. 2011. pH regulation and beyond: unanticipated functions for the voltage-gated proton channel, HVCN1. *Trends Cell Biol.* 21:20–28. http://dx.doi.org/10.1016/j.tcb.2010.09.006

Chamberlin, A., F. Qiu, S. Rebolledo, Y. Wang, S.Y. Noskov, and H.P. Larsson. 2014. Hydrophobic plug functions as a gate in voltage-gated proton channels. *Proc. Natl. Acad. Sci. USA.* 111:E273–E282. http://dx.doi.org/10.1073/pnas.1318018111

Chamberlin, A., F. Qiu, Y. Wang, S.Y. Noskov, and H.P. Larsson. 2015. Mapping the gating and permeation pathways in the voltage-gated proton channel Hv1. *J. Mol. Biol.* 427:131–145. http://dx.doi.org/10.1016/j.jmb.2014.11.018

Chaves, G., C. Derst, A. Franzen, Y. Mashimo, R. Machida, and B. Musset. 2016. Identification of an H_V1 voltage-gated proton channel in insects. *FEBS J.* 283:1453–1464. http://dx.doi.org/10.1111/febs.13680

Chen, K., J. Hirst, R. Camba, C.A. Bonagura, C.D. Stout, B.K. Burgess, and F.A. Armstrong. 2000. Atomically defined mechanism for proton transfer to a buried redox centre in a protein. *Nature.* 405:814–817. http://dx.doi.org/10.1038/35015610

Cherny, V.V., and T.E. DeCoursey. 1999. pH-dependent inhibition of voltage-gated H^+ currents in rat alveolar epithelial cells by Zn^{2+} and other divalent cations. *J. Gen. Physiol.* 114:819–838. http://dx.doi.org/10.1085/jgp.114.6.819

Cherny, V.V., V.S. Markin, and T.E. DeCoursey. 1995. The voltage-activated hydrogen ion conductance in rat alveolar epithelial cells is determined by the pH gradient. *J. Gen. Physiol.* 105:861–896. http://dx.doi.org/10.1085/jgp.105.6.861

Cherny, V.V., L.M. Henderson, and T.E. DeCoursey. 1997. Proton and chloride currents in Chinese hamster ovary cells. *Membr. Cell Biol.* 11:337–347.

Cherny, V.V., L.M. Henderson, W. Xu, L.L. Thomas, and T.E. DeCoursey. 2001. Activation of NADPH oxidase-related proton and electron currents in human eosinophils by arachidonic acid. *J. Physiol.* 535:783–794. http://dx.doi.org/10.1111/j.1469-7793.2001.00783.x

Cherny, V.V., D. Morgan, B. Musset, G. Chaves, S.M.E. Smith, and T.E. DeCoursey. 2015. Tryptophan 207 is crucial to the unique properties of the human voltage-gated proton channel, hH_V1. *J. Gen. Physiol.* 146:343–356. http://dx.doi.org/10.1085/jgp.201511456

Cornish, A.J., K. Gärtner, H. Yang, J.W. Peters, and E.L. Hegg. 2011. Mechanism of proton transfer in [FeFe]-hydrogenase from *Clostridium pasteurianum*. *J. Biol. Chem.* 286:38341–38347. http://dx.doi.org/10.1074/jbc.M111.254664

Courtenay, E.S., M.W. Capp, and M.T. Record Jr. 2001. Thermodynamics of interactions of urea and guanidinium salts with protein surface: relationship between solute effects on protein processes and changes in water-accessible surface area. *Protein Sci.* 10:2485–2497. http://dx.doi.org/10.1110/ps.ps.20801

DeCoursey, T.E. 1991. Hydrogen ion currents in rat alveolar epithelial cells. *Biophys. J.* 60:1243–1253. http://dx.doi.org/10.1016/S0006-3495(91)82158-0

DeCoursey, T.E. 2003a. Interactions between NADPH oxidase and voltage-gated proton channels: why electron transport depends on proton transport. *FEBS Lett.* 555:57–61. http://dx.doi.org/10.1016/S0014-5793(03)01103-7

DeCoursey, T.E. 2003b. Voltage-gated proton channels and other proton transfer pathways. *Physiol. Rev.* 83:475–579. http://dx.doi.org/10.1152/physrev.00028.2002

DeCoursey, T.E. 2010. Voltage-gated proton channels find their dream job managing the respiratory burst in phagocytes. *Physiology (Bethesda).* 25:27–40. http://dx.doi.org/10.1152/physiol.00039.2009

DeCoursey, T.E. 2012. Voltage-gated proton channels. *Compr. Physiol.* 2:1355–1385.

DeCoursey, T.E. 2013. Voltage-gated proton channels: molecular biology, physiology, and pathophysiology of the H_V family. *Physiol. Rev.* 93:599–652. http://dx.doi.org/10.1152/physrev.00011.2012

DeCoursey, T.E. 2015a. Structural revelations of the human proton channel. *Proc. Natl. Acad. Sci. USA.* 112:13430–13431. http://dx.doi.org/10.1073/pnas.1518486112

DeCoursey, T.E. 2015b. The voltage-gated proton channel: a riddle, wrapped in a mystery, inside an enigma. *Biochemistry.* 54:3250–3268. http://dx.doi.org/10.1021/acs.biochem.5b00353

DeCoursey, T.E. 2016. The intimate and controversial relationship between voltage gated proton channels and the phagocyte NAD PH oxidase. *Immunol. Rev.* In press.

DeCoursey, T.E., and V.V. Cherny. 1993. Potential, pH, and arachidonate gate hydrogen ion currents in human neutrophils.

Downloaded from http://rupress.org/jgp/article-pdf/148/2/97/1795854/jgp_201611619.pdf by guest on 08 February 2026

Biophys. J. 65:1590–1598. http://dx.doi.org/10.1016/S0006-3495(93)81198-6

DeCoursey, T.E., and V.V. Cherny. 1994. Voltage-activated hydrogen ion currents. *J. Membr. Biol.* 141:203–223. http://dx.doi.org/10.1007/BF00235130

DeCoursey, T.E., and V.V. Cherny. 1996. Effects of buffer concentration on voltage-gated H^+ currents: does diffusion limit the conductance? *Biophys. J.* 71:182–193. http://dx.doi.org/10.1016/S0006-3495(96)79215-9

DeCoursey, T.E., and V.V. Cherny. 1997. Deuterium isotope effects on permeation and gating of proton channels in rat alveolar epithelium. *J. Gen. Physiol.* 109:415–434. http://dx.doi.org/10.1085/jgp.109.4.415

DeCoursey, T.E., and V.V. Cherny. 1998. Temperature dependence of voltage-gated H^+ currents in human neutrophils, rat alveolar epithelial cells, and mammalian phagocytes. *J. Gen. Physiol.* 112:503–522. http://dx.doi.org/10.1085/jgp.112.4.503

DeCoursey, T.E., and J. Hosler. 2014. Philosophy of voltage-gated proton channels. *J. R. Soc. Interface.* 11:20130799. http://dx.doi.org/10.1098/rsif.2013.0799

DeCoursey, T.E., V.V. Cherny, W. Zhou, and L.L. Thomas. 2000. Simultaneous activation of NADPH oxidase-related proton and electron currents in human neutrophils. *Proc. Natl. Acad. Sci. USA.* 97:6885–6889. http://dx.doi.org/10.1073/pnas.100047297

DeCoursey, T.E., V.V. Cherny, A.G. DeCoursey, W. Xu, and L.L. Thomas. 2001a. Interactions between NADPH oxidase-related proton and electron currents in human eosinophils. *J. Physiol.* 535:767–781. http://dx.doi.org/10.1111/j.1469-7793.2001.00767.x

DeCoursey, T.E., V.V. Cherny, D. Morgan, B.Z. Katz, and M.C. Dinauer. 2001b. The gp91^{phox} component of NADPH oxidase is not the voltage-gated proton channel in phagocytes, but it helps. *J. Biol. Chem.* 276:36063–36066. http://dx.doi.org/10.1074/jbc.C100352200

DeCoursey, T.E., D. Morgan, and V.V. Cherny. 2002. The gp91^{phox} component of NADPH oxidase is not a voltage-gated proton channel. *J. Gen. Physiol.* 120:773–779. http://dx.doi.org/10.1085/jgp.20028704

DeCoursey, T.E., D. Morgan, and V.V. Cherny. 2003. The voltage dependence of NADPH oxidase reveals why phagocytes need proton channels. *Nature.* 422:531–534. http://dx.doi.org/10.1038/nature01523

Demaurex, N. 2012. Functions of proton channels in phagocytes. *Wiley Interdiscip. Rev. Membr. Transp. Signal.* 1:3–15. http://dx.doi.org/10.1002/wmts.2

Doroshenko, P.A., P.G. Kostyuk, and A.E. Martynyuk. 1986. Transmembrane outward hydrogen current in intracellularly perfused neurones of the snail *Helix pomatia*. *Gen. Physiol. Biophys.* 5:337–350.

Dudev, T., B. Musset, D. Morgan, V.V. Cherny, S.M.E. Smith, K. Mazmanian, T.E. DeCoursey, and C. Lim. 2015. Selectivity mechanism of the voltage-gated proton channel, H_V1. *Sci. Rep.* 5:10320. http://dx.doi.org/10.1038/srep10320

Eder, C., and T.E. DeCoursey. 2001. Voltage-gated proton channels in microglia. *Prog. Neurobiol.* 64:277–305. http://dx.doi.org/10.1016/S0301-0082(00)00062-9

El Chemaly, A., Y. Okochi, M. Sasaki, S. Arnaudeau, Y. Okamura, and N. Demaurex. 2010. VSOP/Hv1 proton channels sustain calcium entry, neutrophil migration, and superoxide production by limiting cell depolarization and acidification. *J. Exp. Med.* 207:129–139. http://dx.doi.org/10.1084/jem.20091837

England, J.L., and G. Haran. 2011. Role of solvation effects in protein denaturation: from thermodynamics to single molecules and back. *Annu. Rev. Phys. Chem.* 62:257–277. http://dx.doi.org/10.1146/annurev-physchem-032210-103531

Fillingame, R.H., C.M. Angevine, and O.Y. Dmitriev. 2002. Coupling proton movements to *c*-ring rotation in F_1F_o ATP synthase: aqueous access channels and helix rotations at the *a-c* interface. *Biochim. Biophys. Acta.* 1555:29–36. http://dx.doi.org/10.1016/S0005-2728(02)00250-5

Fischer, H. 2012. Function of proton channels in lung epithelia. *Wiley Interdiscip. Rev. Membr. Transp. Signal.* 1:247–258. http://dx.doi.org/10.1002/wmts.17

Fujiwara, Y., T. Kurokawa, K. Takeshita, M. Kobayashi, Y. Okochi, A. Nakagawa, and Y. Okamura. 2012. The cytoplasmic coiled-coil mediates cooperative gating temperature sensitivity in the voltage-gated H^+ channel Hv1. *Nat. Commun.* 3:816. http://dx.doi.org/10.1038/ncomms1823

Fujiwara, Y., T. Kurokawa, K. Takeshita, A. Nakagawa, H.P. Larsson, and Y. Okamura. 2013a. Gating of the designed trimeric/tetrameric voltage-gated H^+ channel. *J. Physiol.* 591:627–640. http://dx.doi.org/10.1113/jphysiol.2012.243006

Fujiwara, Y., K. Takeshita, A. Nakagawa, and Y. Okamura. 2013b. Structural characteristics of the redox-sensing coiled coil in the voltage-gated H^+ channel. *J. Biol. Chem.* 288:17968–17975. http://dx.doi.org/10.1074/jbc.M113.459024

Fujiwara, Y., T. Kurokawa, and Y. Okamura. 2014. Long α helices projecting from the membrane as the dimer interface in the voltage-gated H^+ channel. *J. Gen. Physiol.* 143:377–386. http://dx.doi.org/10.1085/jgp.201311082

Gonzalez, C., H.P. Koch, B.M. Drum, and H.P. Larsson. 2010. Strong cooperativity between subunits in voltage-gated proton channels. *Nat. Struct. Mol. Biol.* 17:51–56. http://dx.doi.org/10.1038/nsmb.1739

Gonzalez, C., S. Rebolledo, M.E. Perez, and H.P. Larsson. 2013. Molecular mechanism of voltage sensing in voltage-gated proton channels. *J. Gen. Physiol.* 141:275–285. http://dx.doi.org/10.1085/jgp.201210857

Henderson, L.M. 1998. Role of histidines identified by mutagenesis in the NADPH oxidase-associated H^+ channel. *J. Biol. Chem.* 273:33216–33223. http://dx.doi.org/10.1074/jbc.273.50.33216

Henderson, L.M., and J.B. Chappell. 1992. The NADPH-oxidase-associated H^+ channel is opened by arachidonate. *Biochem. J.* 283:171–175. http://dx.doi.org/10.1042/bj2830171

Henderson, L.M., and J.B. Chappell. 1996. NADPH oxidase of neutrophils. *Biochim. Biophys. Acta.* 1273:87–107. http://dx.doi.org/10.1016/0005-2728(95)00140-9

Henderson, L.M., and R.W. Meech. 1999. Evidence that the product of the human X-linked CGD gene, gp91-*phox*, is a voltage-gated H^+ pathway. *J. Gen. Physiol.* 114:771–786. http://dx.doi.org/10.1085/jgp.114.6.771

Henderson, L.M., and R.W. Meech. 2002. Proton conduction through gp91^{phox}. *J. Gen. Physiol.* 120:759–765. http://dx.doi.org/10.1085/jgp.20028708

Henderson, L.M., J.B. Chappell, and O.T.G. Jones. 1987. The superoxide-generating NADPH oxidase of human neutrophils is electrogenic and associated with an H^+ channel. *Biochem. J.* 246:325–329. http://dx.doi.org/10.1042/bj2460325

Henderson, L.M., J.B. Chappell, and O.T.G. Jones. 1988. Superoxide generation by the electrogenic NADPH oxidase of human neutrophils is limited by the movement of a compensating charge. *Biochem. J.* 255:285–290.

Henderson, L.M., G. Banting, and J.B. Chappell. 1995. The arachidonate-activable, NADPH oxidase-associated H^+ channel. Evidence that gp91-*phox* functions as an essential part of the channel. *J. Biol. Chem.* 270:5909–5916. http://dx.doi.org/10.1074/jbc.270.11.5909

Henderson, L.M., S. Thomas, G. Banting, and J.B. Chappell. 1997. The arachidonate-activatable, NADPH oxidase-associated H^+ channel is contained within the multi-membrane-spanning

Downloaded from http://rupress.org/jgp/article-pdf/148/2/97/1795854/jgp_201611619.pdf by guest on 08 February 2026

N-terminal region of gp91-*phox*. *Biochem. J.* 325:701–705. http://dx.doi.org/10.1042/bj3250701

Hodgkin, A.L., and A.F. Huxley. 1952. A quantitative description of membrane current and its application to conduction and excitation in nerve. *J. Physiol.* 117:500–544. http://dx.doi.org/10.1113/jphysiol.1952.sp004764

Hondares, E., M.A. Brown, B. Musset, D. Morgan, V.V. Cherny, C. Taubert, M.K. Bhamrah, D. Coe, F. Marelli-Berg, J.G. Gribben, et al. 2014. Enhanced activation of an amino-terminally truncated isoform of the voltage-gated proton channel HVCN1 enriched in malignant B cells. *Proc. Natl. Acad. Sci. USA.* 111:18078–18083. http://dx.doi.org/10.1073/pnas.1411390111

Hong, L., M.M. Pathak, I.H. Kim, D. Ta, and F. Tombola. 2013. Voltage-sensing domain of voltage-gated proton channel Hv1 shares mechanism of block with pore domains. *Neuron.* 77:274–287. http://dx.doi.org/10.1016/j.neuron.2012.11.013

Hong, L., I.H. Kim, and F. Tombola. 2014. Molecular determinants of Hv1 proton channel inhibition by guanidine derivatives. *Proc. Natl. Acad. Sci. USA.* 111:9971–9976. http://dx.doi.org/10.1073/pnas.1324012111

Hong, L., V. Singh, H. Wulff, and F. Tombola. 2015. Interrogation of the intersubunit interface of the open Hv1 proton channel with a probe of allosteric coupling. *Sci. Rep.* 5:14077. http://dx.doi.org/10.1038/srep14077

Iovannisci, D., B. Illek, and H. Fischer. 2010. Function of the HVCN1 proton channel in airway epithelia and a naturally occurring mutation, M91T. *J. Gen. Physiol.* 136:35–46. http://dx.doi.org/10.1085/jgp.200910379

Jimenez-Morales, D., J. Liang, and B. Eisenberg. 2012. Ionizable side chains at catalytic active sites of enzymes. *Eur. Biophys. J.* 41:449–460. http://dx.doi.org/10.1007/s00249-012-0798-4

Johns, S.J. 2016. TOPO2. Transmembrane protein display software. http://www.sacs.ucsf.edu/TOPO2 (accessed April 21, 2016).

Kalia, J., and K.J. Swartz. 2011. Elucidating the molecular basis of action of a classic drug: guanidine compounds as inhibitors of voltage-gated potassium channels. *Mol. Pharmacol.* 80:1085–1095. http://dx.doi.org/10.1124/mol.111.074989

Kang, B.E., and B.J. Baker. 2016. Pado, a fluorescent protein with proton channel activity can optically monitor membrane potential, intracellular pH, and map gap junctions. *Sci. Rep.* 6:23865. http://dx.doi.org/10.1038/srep23865

Kapus, A., R. Romanek, and S. Grinstein. 1994. Arachidonic acid stimulates the plasma membrane H^+ conductance of macrophages. *J. Biol. Chem.* 269:4736–4745.

Kawanabe, A., and Y. Okamura. 2016. Effects of unsaturated fatty acids on the kinetics of voltage-gated proton channels heterologously expressed in cultured cells. *J. Physiol.* 594:595–610. http://dx.doi.org/10.1113/JP271274

Killian, J.A., and G. von Heijne. 2000. How proteins adapt to a membrane-water interface. *Trends Biochem. Sci.* 25:429–434. http://dx.doi.org/10.1016/S0968-0004(00)01626-1

Koch, H.P., T. Kurokawa, Y. Okochi, M. Sasaki, Y. Okamura, and H.P. Larsson. 2008. Multimeric nature of voltage-gated proton channels. *Proc. Natl. Acad. Sci. USA.* 105:9111–9116. http://dx.doi.org/10.1073/pnas.0801553105

Kulleperuma, K., S.M.E. Smith, D. Morgan, B. Musset, J. Holyoake, N. Chakrabarti, V.V. Cherny, T.E. DeCoursey, and R. Pomès. 2013. Construction and validation of a homology model of the human voltage-gated proton channel hH_V1. *J. Gen. Physiol.* 141:445–465. http://dx.doi.org/10.1085/jgp.201210856

Kuno, M., H. Ando, H. Morihata, H. Sakai, H. Mori, M. Sawada, and S. Oiki. 2009. Temperature dependence of proton permeation through a voltage-gated proton channel. *J. Gen. Physiol.* 134:191–205. http://dx.doi.org/10.1085/jgp.200910213

Kurokawa, T., and Y. Okamura. 2014. Mapping of sites facing aqueous environment of voltage-gated proton channel at resting state: a study with PEGylation protection. *Biochim. Biophys. Acta.* 1838:382–387. http://dx.doi.org/10.1016/j.bbamem.2013.10.001

Lacroix, J.J., H.C. Hyde, F.V. Campos, and F. Bezanilla. 2014. Moving gating charges through the gating pore in a Kv channel voltage sensor. *Proc. Natl. Acad. Sci. USA.* 111:E1950–E1959. http://dx.doi.org/10.1073/pnas.1406161111

Landolt-Marticorena, C., K.A. Williams, C.M. Deber, and R.A. Reithmeier. 1993. Non-random distribution of amino acids in the transmembrane segments of human type I single span membrane proteins. *J. Mol. Biol.* 229:602–608. http://dx.doi.org/10.1006/jmbi.1993.1066

Lecar, H., H.P. Larsson, and M. Grabe. 2003. Electrostatic model of S4 motion in voltage-gated ion channels. *Biophys. J.* 85:2854–2864. http://dx.doi.org/10.1016/S0006-3495(03)74708-0

Lee, S.Y., J.A. Letts, and R. Mackinnon. 2008. Dimeric subunit stoichiometry of the human voltage-dependent proton channel Hv1. *Proc. Natl. Acad. Sci. USA.* 105:7692–7695. http://dx.doi.org/10.1073/pnas.0803277105

Letts, J.A. 2014. Functional and structural studies of the human voltage-gated proton channel. PhD thesis. The Rockefeller University, New York. 209 pp.

Li, Q., S. Wanderling, M. Paduch, D. Medovoy, A. Singharoy, R. McGreevy, C.A. Villalba-Galea, R.E. Hulse, B. Roux, K. Schulten, et al. 2014. Structural mechanism of voltage-dependent gating in an isolated voltage-sensing domain. *Nat. Struct. Mol. Biol.* 21:244–252. http://dx.doi.org/10.1038/nsmb.2768

Li, Q., R. Shen, J.S. Treger, S.S. Wanderling, W. Milewski, K. Siwowska, F. Bezanilla, and E. Perozo. 2015. Resting state of the human proton channel dimer in a lipid bilayer. *Proc. Natl. Acad. Sci. USA.* 112:E5926–E5935. http://dx.doi.org/10.1073/pnas.1515043112

Li, S.J., Q. Zhao, Q. Zhou, H. Unno, Y. Zhai, and F. Sun. 2010. The role and structure of the carboxyl-terminal domain of the human voltage-gated proton channel Hv1. *J. Biol. Chem.* 285:12047–12054. http://dx.doi.org/10.1074/jbc.M109.040360

Lishko, P.V., I.L. Botchkina, A. Fedorenko, and Y. Kirichok. 2010. Acid extrusion from human spermatozoa is mediated by flagellar voltage-gated proton channel. *Cell.* 140:327–337. http://dx.doi.org/10.1016/j.cell.2009.12.053

Lishko, P.V., Y. Kirichok, D. Ren, B. Navarro, J.J. Chung, and D.E. Clapham. 2012. The control of male fertility by spermatozoan ion channels. *Annu. Rev. Physiol.* 74:453–475. http://dx.doi.org/10.1146/annurev-physiol-020911-153258

Luoto, H.H., E. Nordbo, A.A. Baykov, R. Lahti, and A.M. Malinen. 2013. Membrane Na^+-pyrophosphatases can transport protons at low sodium concentrations. *J. Biol. Chem.* 288:35489–35499. http://dx.doi.org/10.1074/jbc.M113.510909

Mahaut-Smith, M.P. 1989. The effect of zinc on calcium and hydrogen ion currents in intact snail neurones. *J. Exp. Biol.* 145:455–464.

Makhatadze, G.I., and P.L. Privalov. 1992. Protein interactions with urea and guanidinium chloride: A calorimetric study. *J. Mol. Biol.* 226:491–505. http://dx.doi.org/10.1016/0022-2836(92)90963-K

Maturana, A., K.H. Krause, and N. Demaurex. 2002. NOX family NADPH oxidases: Do they have built-in proton channels? *J. Gen. Physiol.* 120:781–786. http://dx.doi.org/10.1085/jgp.20028713

Miller, M.J., M. Oldenburg, and R.H. Fillingame. 1990. The essential carboxyl group in subunit c of the F_1F_0 ATP synthase can be moved and H^+-translocating function retained. *Proc. Natl. Acad. Sci. USA.* 87:4900–4904. http://dx.doi.org/10.1073/pnas.87.13.4900

Downloaded from http://rupress.org/jgp/article-pdf/148/2/97/1795854/jgp_201611619.pdf by guest on 08 February 2026

Mony, L., T.K. Berger, and E.Y. Isacoff. 2015. A specialized molecular motion opens the Hv1 voltage-gated proton channel. *Nat. Struct. Mol. Biol.* 22:283–290. http://dx.doi.org/10.1038/nsmb.2978

Morgan, D., V.V. Cherny, A. Finnegan, J. Bollinger, M.H. Gelb, and T.E. DeCoursey. 2007. Sustained activation of proton channels and NADPH oxidase in human eosinophils and murine granulocytes requires PKC but not $cPLA_2$ α activity. *J. Physiol.* 579:327–344. http://dx.doi.org/10.1113/jphysiol.2006.124248

Morgan, D., M. Capasso, B. Musset, V.V. Cherny, E. Ríos, M.J.S. Dyer, and T.E. DeCoursey. 2009. Voltage-gated proton channels maintain pH in human neutrophils during phagocytosis. *Proc. Natl. Acad. Sci. USA.* 106:18022–18027. http://dx.doi.org/10.1073/pnas.0905565106

Morgan, D., B. Musset, K. Kulleperuma, S.M.E. Smith, S. Rajan, V.V. Cherny, R. Pomès, and T.E. DeCoursey. 2013. Peregrination of the selectivity filter delineates the pore of the human voltage-gated proton channel hH_V1. *J. Gen. Physiol.* 142:625–640. http://dx.doi.org/10.1085/jgp.201311045

Murphy, R., and T.E. DeCoursey. 2006. Charge compensation during the phagocyte respiratory burst. *Biochim. Biophys. Acta.* 1757:996–1011. http://dx.doi.org/10.1016/j.bbabio.2006.01.005

Musset, B., V.V. Cherny, D. Morgan, Y. Okamura, I.S. Ramsey, D.E. Clapham, and T.E. DeCoursey. 2008a. Detailed comparison of expressed and native voltage-gated proton channel currents. *J. Physiol.* 586:2477–2486. http://dx.doi.org/10.1113/jphysiol.2007.149427

Musset, B., D. Morgan, V.V. Cherny, D.W. MacGlashan Jr., L.L. Thomas, E. Ríos, and T.E. DeCoursey. 2008b. A pH-stabilizing role of voltage-gated proton channels in IgE-mediated activation of human basophils. *Proc. Natl. Acad. Sci. USA.* 105:11020–11025. http://dx.doi.org/10.1073/pnas.0800886105

Musset, B., V.V. Cherny, D. Morgan, and T.E. DeCoursey. 2009. The intimate and mysterious relationship between proton channels and NADPH oxidase. *FEBS Lett.* 583:7–12. http://dx.doi.org/10.1016/j.febslet.2008.12.005

Musset, B., M. Capasso, V.V. Cherny, D. Morgan, M. Bhamrah, M.J.S. Dyer, and T.E. DeCoursey. 2010a. Identification of Thr^{29} as a critical phosphorylation site that activates the human proton channel *Hvcn1* in leukocytes. *J. Biol. Chem.* 285:5117–5121. http://dx.doi.org/10.1074/jbc.C109.082727

Musset, B., S.M.E. Smith, S. Rajan, V.V. Cherny, S. Sujai, D. Morgan, and T.E. DeCoursey. 2010b. Zinc inhibition of monomeric and dimeric proton channels suggests cooperative gating. *J. Physiol.* 588:1435–1449. http://dx.doi.org/10.1113/jphysiol.2010.188318

Musset, B., S.M.E. Smith, S. Rajan, V.V. Cherny, D. Morgan, and T.E. DeCoursey. 2010c. Oligomerization of the voltage-gated proton channel. *Channels (Austin).* 4:260–265. http://dx.doi.org/10.4161/chan.4.4.12789

Musset, B., S.M.E. Smith, S. Rajan, D. Morgan, V.V. Cherny, and T.E. DeCoursey. 2011. Aspartate 112 is the selectivity filter of the human voltage-gated proton channel. *Nature.* 480:273–277. http://dx.doi.org/10.1038/nature10557

Okamura, Y., Y. Fujiwara, and S. Sakata. 2015. Gating mechanisms of voltage-gated proton channels. *Annu. Rev. Biochem.* 84:685–709. http://dx.doi.org/10.1146/annurev-biochem-060614-034307

Okuda, H., Y. Yonezawa, Y. Takano, Y. Okamura, and Y. Fujiwara. 2016. Direct interaction between the voltage sensors produces cooperative sustained deactivation in voltage-gated H^+ channel dimers. *J. Biol. Chem.* 291:5935–5947. http://dx.doi.org/10.1074/jbc.M115.666834

Papazian, D.M., X.M. Shao, S.A. Seoh, A.F. Mock, Y. Huang, and D.H. Wainstock. 1995. Electrostatic interactions of S4 voltage sensor in Shaker K^+ channel. *Neuron.* 14:1293–1301. http://dx.doi.org/10.1016/0896-6273(95)90276-7

Pless, S.A., J.D. Galpin, A.P. Niciforovic, and C.A. Ahern. 2011. Contributions of counter-charge in a potassium channel voltage-sensor domain. *Nat. Chem. Biol.* 7:617–623. http://dx.doi.org/10.1038/nchembio.622

Qiu, F., S. Rebolledo, C. Gonzalez, and H.P. Larsson. 2013. Subunit interactions during cooperative opening of voltage-gated proton channels. *Neuron.* 77:288–298. http://dx.doi.org/10.1016/j.neuron.2012.12.021

Ramsey, I.S., M.M. Moran, J.A. Chong, and D.E. Clapham. 2006. A voltage-gated proton-selective channel lacking the pore domain. *Nature.* 440:1213–1216. http://dx.doi.org/10.1038/nature04700

Ramsey, I.S., Y. Mokrab, I. Carvacho, Z.A. Sands, M.S.P. Sansom, and D.E. Clapham. 2010. An aqueous H^+ permeation pathway in the voltage-gated proton channel Hv1. *Nat. Struct. Mol. Biol.* 17:869–875. http://dx.doi.org/10.1038/nsmb.1826

Robinson, R.A., and R.H. Stokes. 1959. Electrolyte Solutions, the Measurement and Interpretation of Conductance, Chemical Potential, and Diffusion in Solutions of Simple Electrolytes. Second edition. Butterworths Scientific Publications, London. 559 pp.

Rodriguez, J.D., S. Haq, K.F. Nowak, D. Morgan, V.V. Cherny, S. Bernstein, M.S. Sapp, J.R. Curcuru, C. Antchouey, S.J. Nowak, et al. 2015. Characterization and subcellular localization of H_V1 in *Lingulodinium polyedrum* confirms its role in bioluminescence. *Biophys. J.* 108:425a. http://dx.doi.org/10.1016/j.bpj.2014.11.2325

Ruivo, R., G.C. Bellenchi, X. Chen, G. Zifarelli, C. Sagné, C. Debacker, M. Pusch, S. Supplisson, and B. Gasnier. 2012. Mechanism of proton/substrate coupling in the heptahelical lysosomal transporter cystinosin. *Proc. Natl. Acad. Sci. USA.* 109:E210–E217. http://dx.doi.org/10.1073/pnas.1115581109

Sakata, S., T. Kurokawa, M.H. Nørholm, M. Takagi, Y. Okochi, G. von Heijne, and Y. Okamura. 2010. Functionality of the voltage-gated proton channel truncated in S4. *Proc. Natl. Acad. Sci. USA.* 107:2313–2318. http://dx.doi.org/10.1073/pnas.0911868107

Sasaki, M., M. Takagi, and Y. Okamura. 2006. A voltage sensor-domain protein is a voltage-gated proton channel. *Science.* 312:589–592. http://dx.doi.org/10.1126/science.1122352

Seredenina, T., N. Demaurex, and K.H. Krause. 2015. Voltage-gated proton channels as novel drug targets: From NADPH oxidase regulation to sperm biology. *Antioxid. Redox Signal.* 23:490–513. http://dx.doi.org/10.1089/ars.2013.5806

Sigg, D., and F. Bezanilla. 1997. Total charge movement per channel. The relation between gating charge displacement and the voltage sensitivity of activation. *J. Gen. Physiol.* 109:27–39. http://dx.doi.org/10.1085/jgp.109.1.27

Smith, S.M.E., and T.E. DeCoursey. 2013. Consequences of dimerization of the voltage-gated proton channel. *Prog. Mol. Biol. Transl. Sci.* 117:335–360. http://dx.doi.org/10.1016/B978-0-12-386931-9.00012-X

Smith, S.M.E., D. Morgan, B. Musset, V.V. Cherny, A.R. Place, J.W. Hastings, and T.E. DeCoursey. 2011. Voltage-gated proton channel in a dinoflagellate. *Proc. Natl. Acad. Sci. USA.* 108:18162–18167. http://dx.doi.org/10.1073/pnas.1115405108

Starace, D.M., and F. Bezanilla. 2001. Histidine scanning mutagenesis of basic residues of the S4 segment of the *Shaker* K^+ channel. *J. Gen. Physiol.* 117:469–490. http://dx.doi.org/10.1085/jgp.117.5.469

Starace, D.M., and F. Bezanilla. 2004. A proton pore in a potassium channel voltage sensor reveals a focused electric field. *Nature.* 427:548–553. http://dx.doi.org/10.1038/nature02270

Downloaded from http://rupress.org/jgp/article-pdf/148/2/97/1795854/jgp_201611619.pdf by guest on 08 February 2026

Suszták, K., A. Mócsai, E. Ligeti, and A. Kapus. 1997. Electrogenic H^+ pathway contributes to stimulus-induced changes of internal pH and membrane potential in intact neutrophils: role of cytoplasmic phospholipase A_2. *Biochem. J.* 325:501–510. http://dx.doi.org/10.1042/bj3250501

Takeshita, K., S. Sakata, E. Yamashita, Y. Fujiwara, A. Kawanabe, T. Kurokawa, Y. Okochi, M. Matsuda, H. Narita, Y. Okamura, and A. Nakagawa. 2014. X-ray crystal structure of voltage-gated proton channel. *Nat. Struct. Mol. Biol.* 21:352–357. http://dx.doi.org/10.1038/nsmb.2783

Tao, X., A. Lee, W. Limapichat, D.A. Dougherty, and R. MacKinnon. 2010. A gating charge transfer center in voltage sensors. *Science.* 328:67–73. http://dx.doi.org/10.1126/science.1185954

Taylor, A.R., A. Chrachri, G. Wheeler, H. Goddard, and C. Brownlee. 2011. A voltage-gated H^+ channel underlying pH homeostasis in calcifying coccolithophores. *PLoS Biol.* 9:e1001085. http://dx.doi.org/10.1371/journal.pbio.1001085

Taylor, A.R., C. Brownlee, and G.L. Wheeler. 2012. Proton channels in algae: reasons to be excited. *Trends Plant Sci.* 17:675–684. http://dx.doi.org/10.1016/j.tplants.2012.06.009

Thomas, R.C., and R.W. Meech. 1982. Hydrogen ion currents and intracellular pH in depolarized voltage-clamped snail neurones. *Nature.* 299:826–828. http://dx.doi.org/10.1038/299826a0

Thorndycroft, F.H., G. Butland, D.J. Richardson, and N.J. Watmough. 2007. A new assay for nitric oxide reductase reveals two conserved glutamate residues form the entrance to a proton-conducting channel in the bacterial enzyme. *Biochem. J.* 401:111–119. http://dx.doi.org/10.1042/BJ20060856

Tiwari-Woodruff, S.K., C.T. Schulteis, A.F. Mock, and D.M. Papazian. 1997. Electrostatic interactions between transmembrane segments mediate folding of Shaker K^+ channel subunits. *Biophys. J.* 72:1489–1500. http://dx.doi.org/10.1016/S0006-3495(97)78797-6

Tombola, F., M.H. Ulbrich, and E.Y. Isacoff. 2008. The voltage-gated proton channel Hv1 has two pores, each controlled by one voltage sensor. *Neuron.* 58:546–556. http://dx.doi.org/10.1016/j.neuron.2008.03.026

Tombola, F., M.H. Ulbrich, S.C. Kohout, and E.Y. Isacoff. 2010. The opening of the two pores of the Hv1 voltage-gated proton channel is tuned by cooperativity. *Nat. Struct. Mol. Biol.* 17:44–50. http://dx.doi.org/10.1038/nsmb.1738

Touret, N., and S. Grinstein. 2002. Voltage-gated proton "channels": a spectator's viewpoint. *J. Gen. Physiol.* 120:767–771. http://dx.doi.org/10.1085/jgp.20028706

Wang, Y., S.J. Li, X. Wu, Y. Che, and Q. Li. 2012. Clinicopathological and biological significance of human voltage-gated proton channel Hv1 protein overexpression in breast cancer. *J. Biol. Chem.* 287:13877–13888. http://dx.doi.org/10.1074/jbc.M112.345280

Wang, Y., X. Wu, Q. Li, S. Zhang, and S.J. Li. 2013. Human voltage-gated proton channel hv1: a new potential biomarker for diagnosis and prognosis of colorectal cancer. *PLoS One.* 8:e70550. http://dx.doi.org/10.1371/journal.pone.0070550

Wood, M.L., E.V. Schow, J.A. Freites, S.H. White, F. Tombola, and D.J. Tobias. 2012. Water wires in atomistic models of the Hv1 proton channel. *Biochim. Biophys. Acta.* 1818:286–293. http://dx.doi.org/10.1016/j.bbamem.2011.07.045

Xu, Q., H.L. Axelrod, E.C. Abresch, M.L. Paddock, M.Y. Okamura, and G. Feher. 2004. X-Ray structure determination of three mutants of the bacterial photosynthetic reaction centers from *Rb. sphaeroides*; altered proton transfer pathways. *Structure.* 12:703–715. http://dx.doi.org/10.1016/j.str.2004.03.001

Yang, N., A.L. George Jr., and R. Horn. 1996. Molecular basis of charge movement in voltage-gated sodium channels. *Neuron.* 16:113–122. http://dx.doi.org/10.1016/S0896-6273(00)80028-8

Yang, N., A.L. George Jr., and R. Horn. 1997. Probing the outer vestibule of a sodium channel voltage sensor. *Biophys. J.* 73:2260–2268. http://dx.doi.org/10.1016/S0006-3495(97)78258-4

Downloaded from http://rupress.org/jgp/article-pdf/148/2/97/1795854/jgp_201611619.pdf by guest on 08 February 2026